Elastic Constants Estimation in Fractured Media (HTI) Using Gauss-Newton Full Waveform Inversion

Authors: Wenyong Pan*, Kris Innanen*, Gary Margrave*, Mike Fehler[†], Xinding Fang[‡], Junxiao Li*

** University of Calgary*

[†] **M. I. T**

[‡] **M. I. T** & ***Chevron***

Motivation

- *Examining the Possibility of Using Full Waveform Inversion Method for Fracture Properties Estimation.*
- **The Limitations of Current Methods for Fracture Characterization.**
  - **Amplitude Method (AVO or AVAZ): Assuming Horizontal Interface**
  - **Travel Time Method: Appropriate for Transmission Survey**
- **The Benefits of Full Waveform Inversion Method.**
  - **Full Wavefields Information (Amplitude, travel time and etc.) for Fracture Properties Estimation**
  - **Overcome the Limitations of Conventional Methods**
- **Estimating Elastic Stiffness Coefficients in Fractured Media (Equivalent HTI Media) Using** ***Multi-parameter Gauss-Newton FWI***

Outline

- Principle of Full Waveform Inversion and Inversion Sensitivity Kernel
- Mono-parameter FWI → Multi-parameter FWI
  - Cross-talk and Parameterization Problems
  - Scattering Patterns and Inversion Sensitivity Analysis
- 3D Fréchet Derivative or Scattering Patterns for General Anisotropic Media: Analytic Results
  - Examining a HTI Case
- Multi-parameter Update and Multi-parameter Hessian with Gauss-Newton Framework
  - Suppressing Cross-talk Using Multi-parameter Hessian
- Numerical Examples
  - Inversion Sensitivity: Analytic vs. Numerical Results (2D)
  - A 2D HTI Case

Review of Full Waveform Inversion and Inversion Sensitivity Kernel

- **Least-squares wave equation inversion:**

$$\phi\left(m(\mathbf{r})\right) = \frac{1}{2}\sum_{\mathbf{r}_s}\sum_{\mathbf{r}_g}\sum_{\omega}\left\|\delta P\left(\mathbf{r}_g, \mathbf{r}_s, \omega\right)\right\|^2$$

- **Model Update:**

$$\delta m\left(\mathbf{r}\right) = -\sum_{\mathbf{r}'} H^{-1}\left(\mathbf{r}, \mathbf{r}'\right) g\left(\mathbf{r}'\right)$$

❖ **Least-squares wave equation inversion:**

$$\phi\left(m(\mathbf{r})\right) = \frac{1}{2}\sum_{\mathbf{r}_s}\sum_{\mathbf{r}_g}\sum_{\omega}\left\|\delta P\left(\mathbf{r}_g,\mathbf{r}_s,\omega\right)\right\|^2$$

❖ **Gradient:**

$$g_n(\mathbf{r}) = \sum_{\mathbf{r}_s}\sum_{\mathbf{r}_g}\sum_{\omega}\Re\left[\underbrace{\frac{\partial u\left(\mathbf{r}_g,\mathbf{r}_s,\omega\right)}{\partial m\left(\mathbf{r}\right)}}_{\text{Fréchet Derivative}}\delta P^*\left(\mathbf{r}_g,\mathbf{r}_s,\omega\right)\right]$$

Fréchet Derivative

❖ **Fréchet derivative or Inversion Sensitivity Kernel:**

$$L(\mathbf{r},\omega)\overbrace{\frac{\partial u(\mathbf{r},\mathbf{r}_s,\omega)}{\partial m(\mathbf{r})}}^{\text{Fréchet Derivative}} = -\underbrace{\frac{\partial L(\mathbf{r},\omega)}{\partial m(\mathbf{r})}}_{\text{Model Perturbation}} u(\mathbf{r},\mathbf{r}_s,\omega)$$

❖ **Approximate Hessian:**

$$\mathbf{H}_a(\mathbf{r},\mathbf{r}') = \underbrace{\frac{\partial u(\mathbf{r}_g,\mathbf{r}_s,\omega)}{\partial m(\mathbf{r})}\frac{\partial u(\mathbf{r}_g,\mathbf{r}_s,\omega)}{\partial m(\mathbf{r}')}}_{\text{Fréchet Derivative}}$$

Mono-parameter FWI → Multi-parameter FWI

- **Mono-parameter FWI:**
  - **Mono parameter *Vp*.**
  - **Cycle-skipping problem (Lack of low frequency, Inaccurate initial model and etc.)**
  - **…………..**

❖ **Multi-parameter FWI:**

- **Cross-talk and parameterization:**
  - **The perturbations of different parameters have coupled effects on the seismic response.**

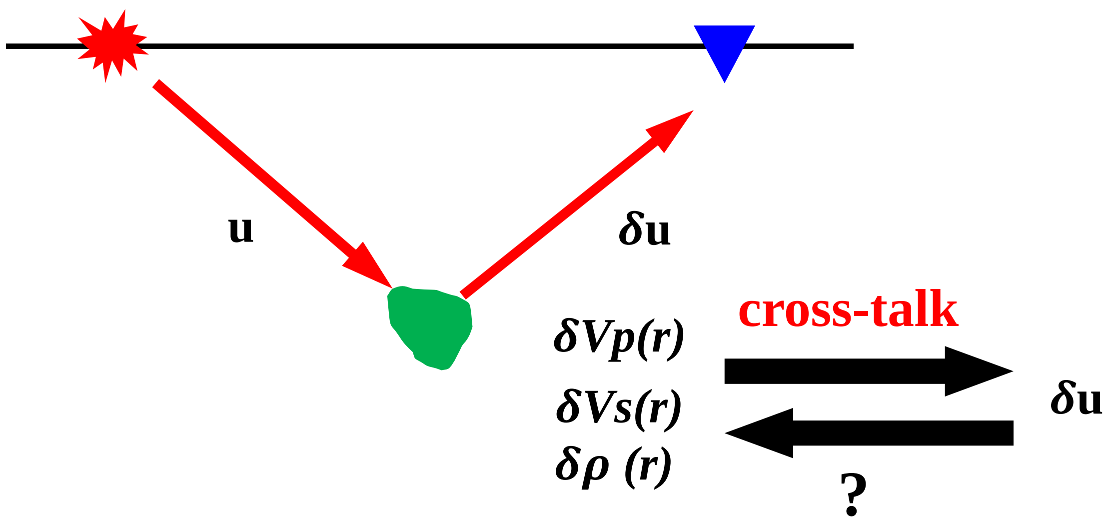

❖ **Multi-parameter FWI:**

- **Cross-talk and parameterization:**
  - **Which parameterization is more suitable for full waveform inversion ?**

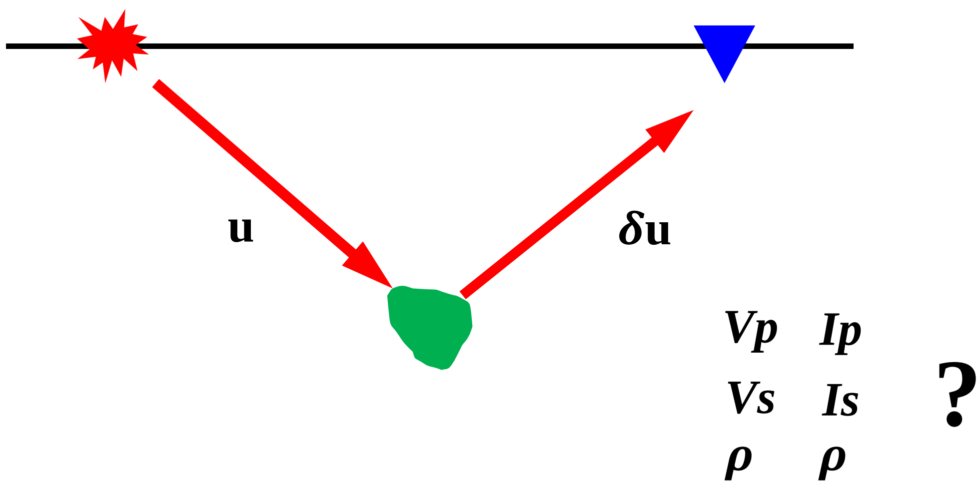

- **Multi-parameter FWI:**
  - **Cross-talk and parameterization:**
    - **How to use multi-offset and multi-azimuth data for effective inversion?**

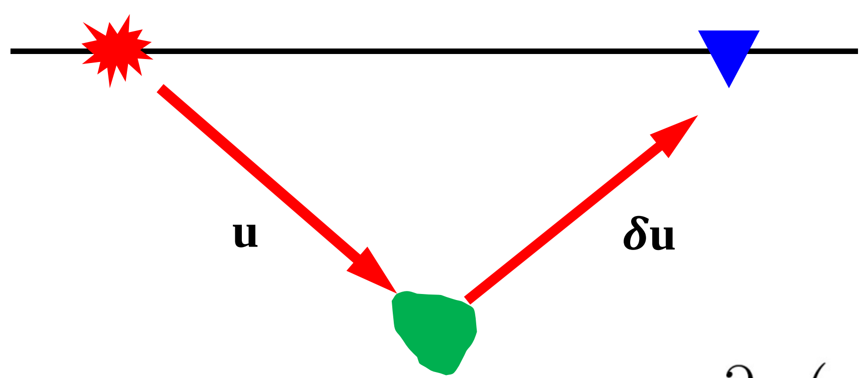

$$\frac{\partial u\left(\mathbf{r}_g, \mathbf{r}_s, \omega\right)}{\partial m\left(\mathbf{r}\right)}$$

Inversion Sensitivity Kernel

Inversion Sensitivity Analysis for multi-parameter FWI: Cross-talk and Scattering Patterns

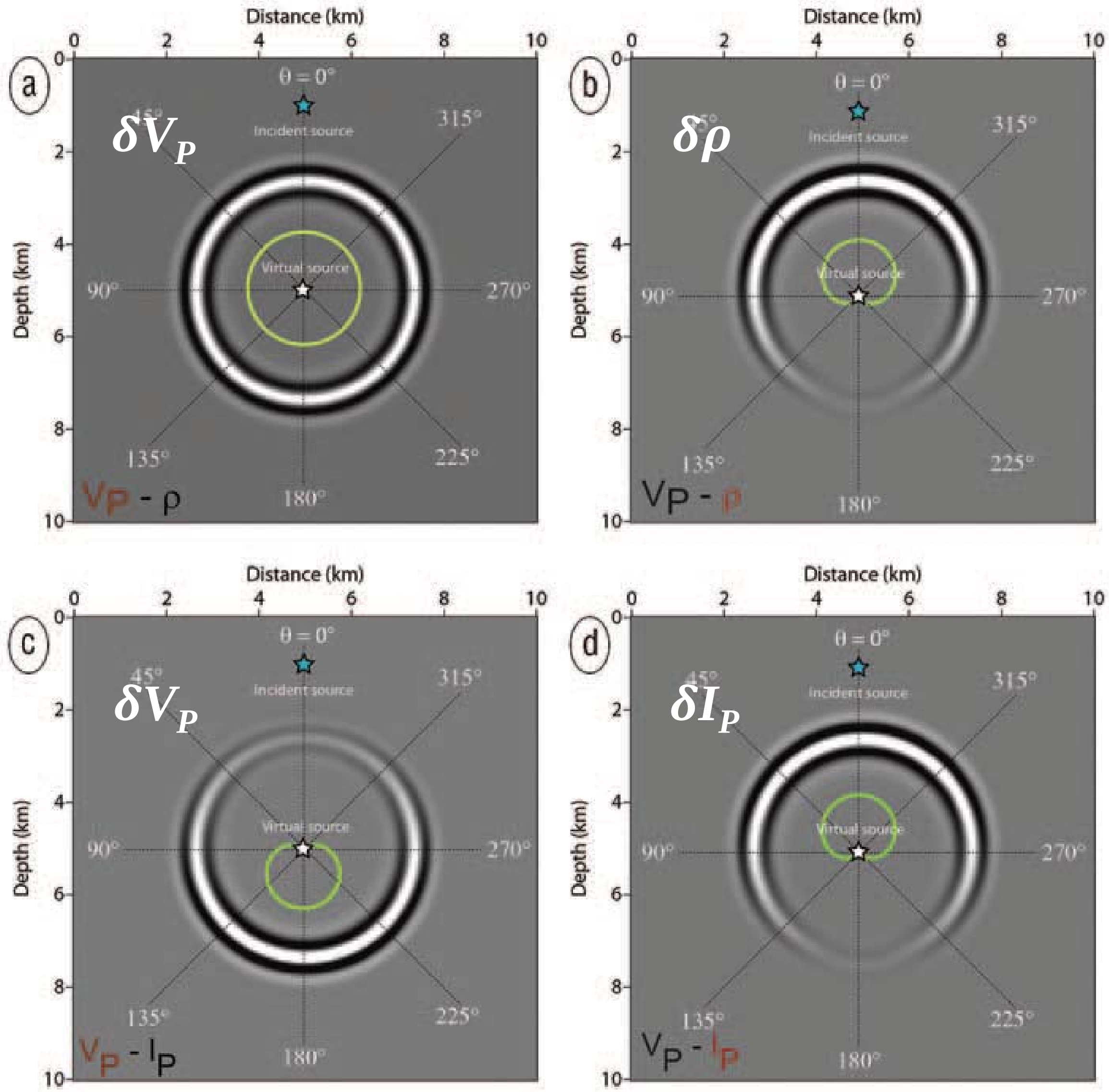

Scattering Patterns for acoustic FWI (Operto et al. , 2013)

3D Fréchet Derivative and Scattering Patterns for General Anisotropic Media: Analytic Results

❖ **Equation of Motion:**

$$\frac{\partial \sigma_{ij}}{\partial x_j} + f_i = \rho \frac{\partial^2 u_i}{\partial t^2}$$

$$\sigma_{ij} = c_{ijkl} \frac{\partial u_k}{\partial x_l}$$

❖ **The Solution of Wavefields:**

$$u_i(\mathbf{r}, \omega) = \int_{\Omega(\mathbf{r}_s)} \int_{\omega_s} f_j(\mathbf{r}_s, \omega_s) G_{ij}(\mathbf{r}, \omega; \mathbf{r}_s, \omega_s) d\Omega(\mathbf{r}_s) d\omega_s$$

❖ **Equation of Motion:**

$$\frac{\partial \sigma_{ij}}{\partial x_j} + f_i = \rho \frac{\partial^2 u_i}{\partial t^2}$$

$$\sigma_{ij} = c_{ijkl} \frac{\partial u_k}{\partial x_l}$$

❖ **Perturbations of Model Parameters:**

$$\delta\rho = \rho - \tilde{\rho}$$

$$\delta c_{ijkl} = c_{ijkl} - \tilde{c}_{ijkl}$$

- **Equation of Motion:**

$$\frac{\partial \sigma_{ij}}{\partial x_j} + f_i = \rho \frac{\partial^2 u_i}{\partial t^2}$$

$$\sigma_{ij} = c_{ijkl} \frac{\partial u_k}{\partial x_l}$$

- **Perturbation of Wavefields:**

$$\delta \mathbf{u} = \mathbf{u} - \tilde{\mathbf{u}}$$

❖ **The Equation Describes the Propagation of Scattered Wavefields (Born Approximation):**

$$\delta M_{ij} = \delta c_{ijkl} \frac{\partial \tilde{u}_k}{\partial x_l}$$

Scattered Wavefields

$$\frac{\partial}{\partial x_j}\left(\tilde{c}_{ijkl}\frac{\partial \delta u_k}{\partial x_l}\right) - \tilde{\rho}\frac{\partial^2 \delta u_i}{\partial t^2} = \underbrace{\delta\rho\frac{\partial^2 \tilde{u}_i}{\partial t^2} - \frac{\partial \delta M_{ij}}{\partial x_j}}_{\text{Scattered Source}}$$

Scattered Source

❖ **The Equation Describes the Propagation of Scattered Wavefields (Born Approximation):**

$$\delta M_{ij} = \delta c_{ijkl}\frac{\partial \tilde{u}_k}{\partial x_l}$$

Scattered Wavefields

$$\frac{\partial}{\partial x_j}\left(\tilde{c}_{ijkl}\frac{\partial \delta u_k}{\partial x_l}\right) - \tilde{\rho}\frac{\partial^2 \delta u_i}{\partial t^2} = \underbrace{\delta\rho\frac{\partial^2 \tilde{u}_i}{\partial t^2} - \frac{\partial \delta M_{ij}}{\partial x_j}}_{\text{Scattered Source}}$$

Scattered Source

❖ **The Solution of Scattered Wavefields:**

$$\delta\bar{u}_n(\mathbf{r},\omega) \approx -\int_{\Omega(\mathbf{r}')}\int_{\omega'} \delta M_{ij}\frac{\partial \tilde{G}_{ni}(\mathbf{r},\omega;\mathbf{r}',\omega')}{\partial x'_j}d\Omega(\mathbf{r}')d\omega'$$

❖ **The Fréchet Derivative for General Anisotropic Media:**

$$\delta \bar{\mathbf{u}}(\mathbf{r},\omega) = -\frac{i\omega \mathbf{exp}(-ik_{\xi} r)}{4\pi\rho\xi^{3} r}\hat{\mathbf{g}}\underbrace{\left(\hat{\mathbf{g}}^{\dagger}\delta\mathbf{M}\hat{\mathbf{r}}\right)}_{\text{Scattering Pattern}}$$

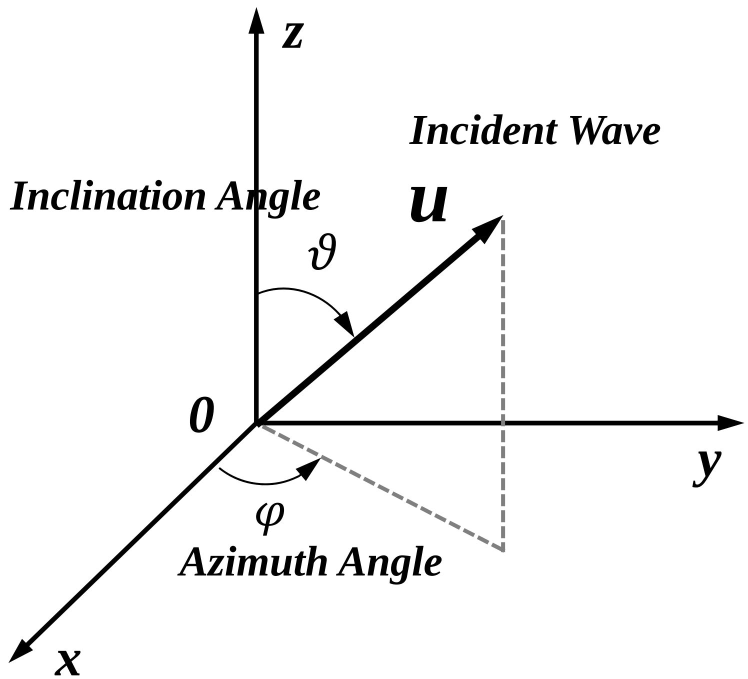

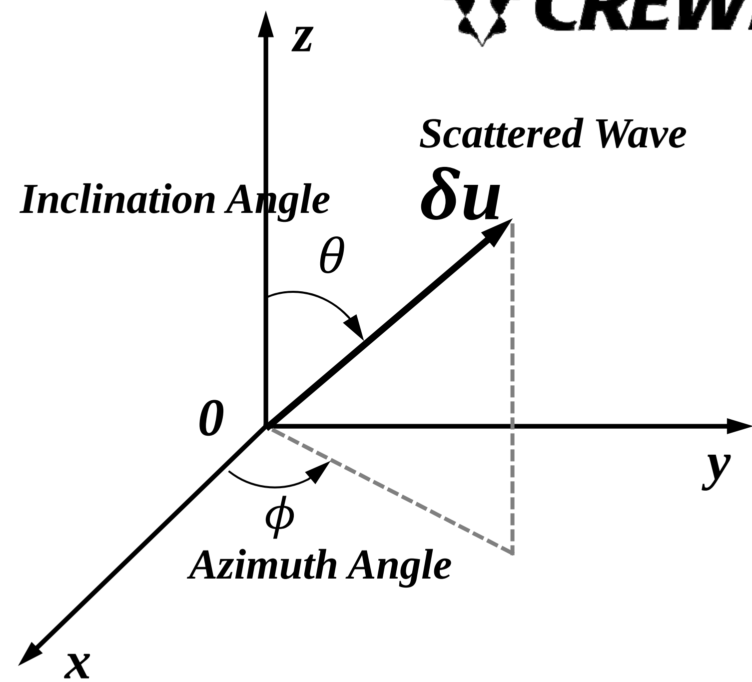

δu: Azimuth angle ϕ, Inclination angle θ

Scattering Coefficients:

$$\mathscr{R}\left(\vartheta,\varphi,\theta,\phi\right)=\hat{\mathbf{g}}^{\dagger}\delta\mathbf{M}\hat{\mathbf{r}}$$

$$\begin{aligned}\hat{\mathbf{r}}^{\dagger}&=[\sin\theta\cos\phi,\sin\theta\sin\phi,\cos\theta],\\ \hat{\theta}^{\dagger}&=[\cos\theta\cos\phi,\cos\theta\sin\phi,-\sin\theta],\\ \hat{\phi}^{\dagger}&=[-\sin\phi,\cos\phi,0].\end{aligned}$$

- **Scattering Pattern for HTI Media:**

$$\mathscr{R}(\vartheta, \varphi, \theta, \phi) = \hat{\mathbf{g}}^{\dagger} \delta \mathbf{M}^{HTI} \hat{\mathbf{r}}$$

- **Moment Tensor Source for HTI media:**

$$\delta \mathbf{M}^{HTI} = \begin{bmatrix} \delta c_{11}\tilde{e}_{11} + \delta c_{13}\tilde{e}_{22} + \delta c_{13}\tilde{e}_{33} & 2\delta c_{55}\tilde{e}_{12} & 2\delta c_{55}\tilde{e}_{13} \\ 2\delta c_{55}\tilde{e}_{12} & \delta c_{13}\tilde{e}_{11} + \delta c_{33}\tilde{e}_{22} + \delta\nu\tilde{e}_{33} & 2\delta c_{44}\tilde{e}_{23} \\ 2\delta c_{55}\tilde{e}_{13} & 2\delta c_{44}\tilde{e}_{23} & \delta c_{13}\tilde{e}_{11} + \delta\nu\tilde{e}_{22} + \delta c_{33}\tilde{e}_{33} \end{bmatrix}$$

3D Scattering Patterns Due to Perturbation of $c_{33.}$ $\vartheta = 0^o, \varphi = 0^o$

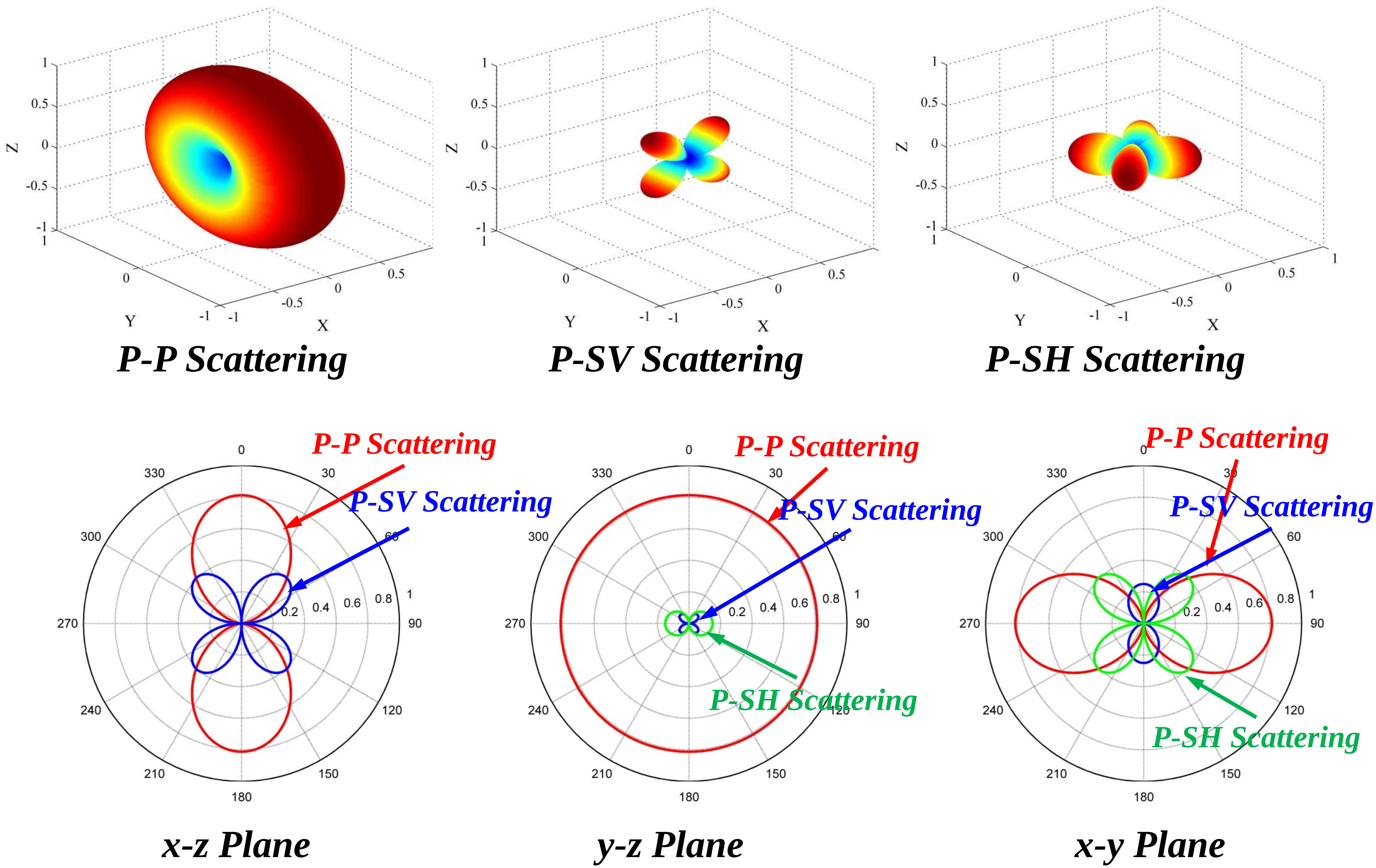

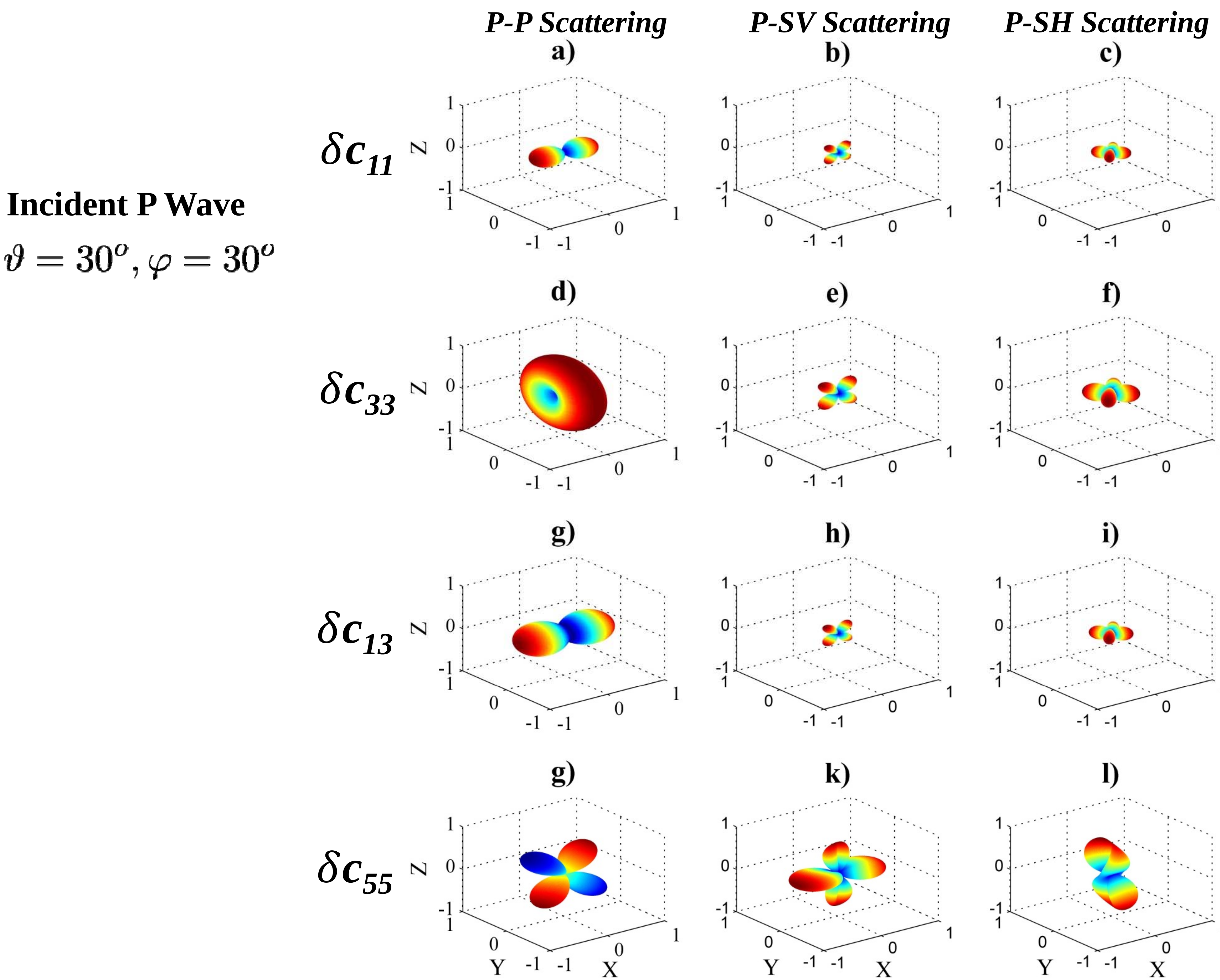

Incident P Wave
$\vartheta = 30^o, \varphi = 30^o$
P-P Scattering
P-SV Scattering
P-SH Scattering
a)
b)
c)
d)
e)
f)
g)
h)
i)
g)
k)
l)
δc_{11}
δc_{33}
δc_{13}
δc_{55}
Z
Y
X

Multi-parameter Update and Multi-parameter Hessian within Gauss-Newton Framework

Multi-parameter Update and Multi-parameter Hessian within Gauss-Newton Framework

$$\begin{bmatrix} \delta c_{33}(\mathbf{r}) \\ \delta c_{55}(\mathbf{r}) \\ \delta c_{11}(\mathbf{r}) \\ \delta c_{13}(\mathbf{r}) \end{bmatrix} = \sum_{\mathbf{r}'} \begin{bmatrix} H_{3333}(\mathbf{r},\mathbf{r}') & H_{3355}(\mathbf{r},\mathbf{r}') & H_{3311}(\mathbf{r},\mathbf{r}') & H_{3313}(\mathbf{r},\mathbf{r}') \\ H_{5533}(\mathbf{r},\mathbf{r}') & H_{5555}(\mathbf{r},\mathbf{r}') & H_{5511}(\mathbf{r},\mathbf{r}') & H_{5513}(\mathbf{r},\mathbf{r}') \\ H_{1133}(\mathbf{r},\mathbf{r}') & H_{1155}(\mathbf{r},\mathbf{r}') & H_{1111}(\mathbf{r},\mathbf{r}') & H_{1113}(\mathbf{r},\mathbf{r}') \\ H_{1333}(\mathbf{r},\mathbf{r}') & H_{1355}(\mathbf{r},\mathbf{r}') & H_{1311}(\mathbf{r},\mathbf{r}') & H_{1313}(\mathbf{r},\mathbf{r}') \end{bmatrix}^{-1} \begin{bmatrix} g_{33}(\mathbf{r}') \\ g_{55}(\mathbf{r}') \\ g_{11}(\mathbf{r}') \\ g_{13}(\mathbf{r}') \end{bmatrix}$$

Multi-parameter Update 2D HTI Case

Multi-parameter Update and Multi-parameter Hessian within Gauss-Newton Framework

$$\tilde{g}_{33}(\mathbf{r}) = \sum_{\mathbf{r}_s} \sum_{\mathbf{r}_g} \sum_{\omega} \Re\left[\frac{\partial u(\mathbf{r}_g, \mathbf{r}_s, \omega)}{\partial c_{33}} \delta P_{33}^{*}(\mathbf{r}_g, \mathbf{r}_s, \omega)\right]$$

Exact Gradient without Cross-talk

Multi-parameter Update and Multi-parameter Hessian within Gauss-Newton Framework

Cross-talk

$$g_{33}(\mathbf{r}) = \sum_{\mathbf{r}_s} \sum_{\mathbf{r}_g} \sum_{\omega} \Re\left[\frac{\partial u(\mathbf{r}_g, \mathbf{r}_s, \omega)}{\partial c_{33}} \left(\delta P_{33}^* + \delta P_{55}^* + \delta P_{11}^* + \delta P_{13}^*\right)\right]$$

Gradient Suffers from Cross-talk

Multi-parameter Update and Multi-parameter Hessian within Gauss-Newton Framework

$$
\mathbf{H}_a\left(\mathbf{r},\mathbf{r}'\right) = \begin{bmatrix}
\frac{\partial^2 u(\mathbf{r}_g,\mathbf{r}_s,\omega)}{\partial c_{33}(\mathbf{r})\partial c_{33}(\mathbf{r}')} & \frac{\partial^2 u(\mathbf{r}_g,\mathbf{r}_s,\omega)}{\partial c_{33}(\mathbf{r}) c_{55}(\mathbf{r}')} & \frac{\partial^2 u(\mathbf{r}_g,\mathbf{r}_s,\omega)}{\partial c_{33}(\mathbf{r})\partial c_{11}(\mathbf{r}')} & \frac{\partial^2 u(\mathbf{r}_g,\mathbf{r}_s,\omega)}{\partial c_{33}(\mathbf{r})\partial c_{11}(\mathbf{r}')} \\
\frac{\partial^2 u(\mathbf{r}_g,\mathbf{r}_s,\omega)}{\partial c_{55}(\mathbf{r})\partial c_{33}(\mathbf{r}')} & \frac{\partial^2 u(\mathbf{r}_g,\mathbf{r}_s,\omega)}{\partial c_{55}(\mathbf{r})\partial c_{55}(\mathbf{r}')} & \frac{\partial^2 u(\mathbf{r}_g,\mathbf{r}_s,\omega)}{\partial c_{55}(\mathbf{r})\partial c_{11}(\mathbf{r}')} & \frac{\partial^2 u(\mathbf{r}_g,\mathbf{r}_s,\omega)}{\partial c_{55}(\mathbf{r})\partial c_{13}(\mathbf{r}')} \\
\frac{\partial^2 u(\mathbf{r}_g,\mathbf{r}_s,\omega)}{\partial c_{11}(\mathbf{r})\partial c_{33}(\mathbf{r}')} & \frac{\partial^2 u(\mathbf{r}_g,\mathbf{r}_s,\omega)}{\partial c_{11}(\mathbf{r})\partial c_{55}(\mathbf{r}')} & \frac{\partial^2 u(\mathbf{r}_g,\mathbf{r}_s,\omega)}{\partial c_{11}(\mathbf{r})\partial c_{11}(\mathbf{r}')} & \frac{\partial^2 u(\mathbf{r}_g,\mathbf{r}_s,\omega)}{\partial c_{11}(\mathbf{r})\partial c_{13}(\mathbf{r}')} \\
\frac{\partial^2 u(\mathbf{r}_g,\mathbf{r}_s,\omega)}{\partial c_{13}(\mathbf{r})\partial c_{33}(\mathbf{r}')} & \frac{\partial^2 u(\mathbf{r}_g,\mathbf{r}_s,\omega)}{\partial c_{13}(\mathbf{r})\partial c_{55}(\mathbf{r}')} & \frac{\partial^2 u(\mathbf{r}_g,\mathbf{r}_s,\omega)}{\partial c_{13}(\mathbf{r})\partial c_{11}(\mathbf{r}')} & \frac{\partial^2 u(\mathbf{r}_g,\mathbf{r}_s,\omega)}{\partial c_{13}(\mathbf{r})\partial c_{13}(\mathbf{r}')}
\end{bmatrix}
$$

Multi-parameter Approximate Hessian Suppresses Cross-talk

Multi-parameter Update and Multi-parameter Hessian within Gauss-Newton Framework

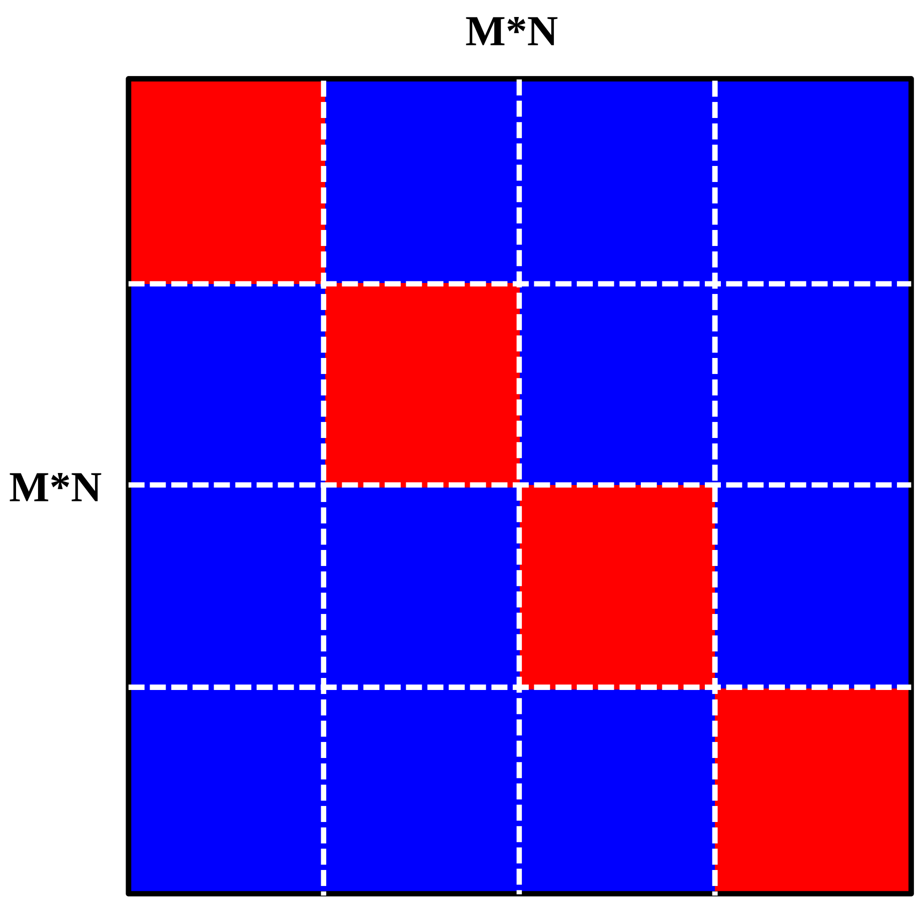

Schematic Diagram of the Multi-parameter Hessian

Multi-parameter Update and Multi-parameter Hessian within Gauss-Newton Framework

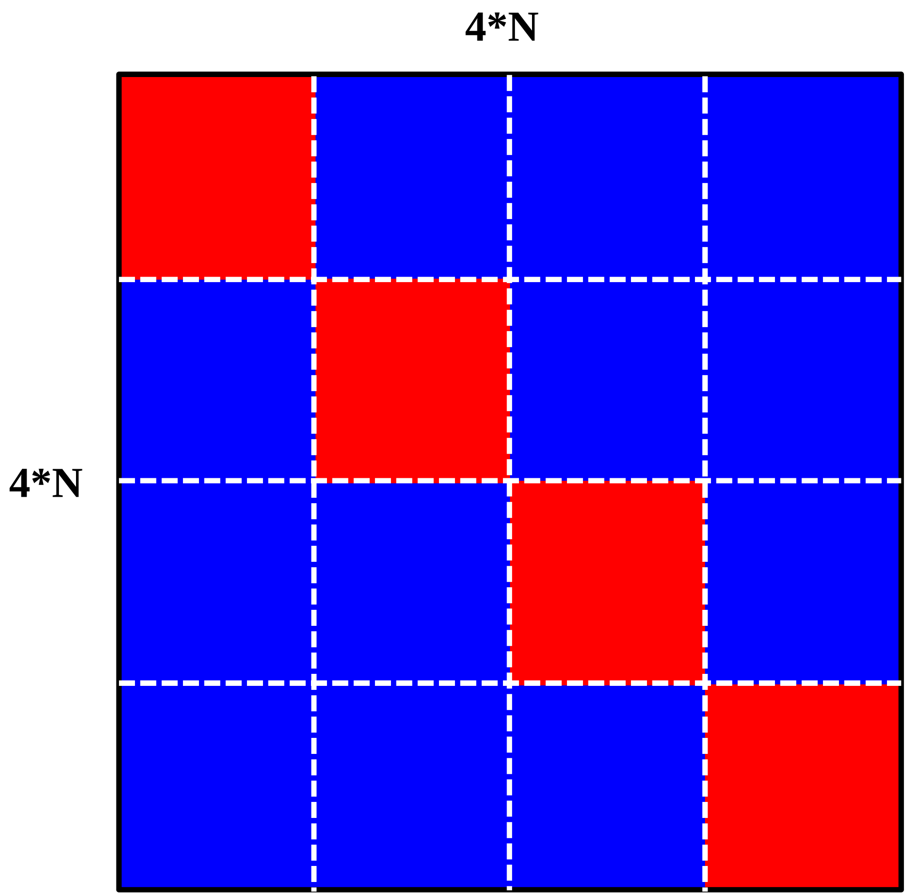

Schematic Diagram of the Multi-parameter Hessian

Multi-parameter Update and Multi-parameter Hessian within Gauss-Newton Framework

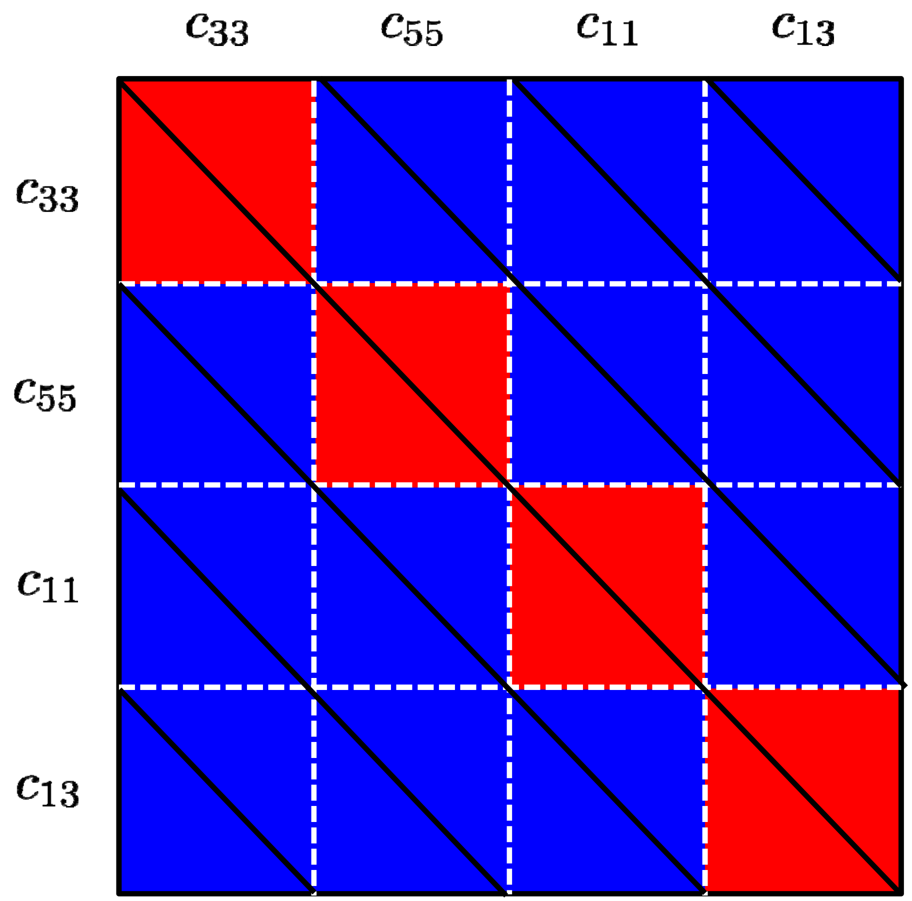

Schematic Diagram of the Multi-parameter Hessian

Multi-parameter Update and Multi-parameter Hessian within Gauss-Newton Framework

$$\bar{\mathbf{H}}_a\left(\mathbf{r},\mathbf{r}'\right) = \begin{bmatrix} \frac{\partial^2 u(\mathbf{r}_g,\mathbf{r}_s,\omega)}{\partial c_{33}(\mathbf{r})\partial c_{33}(\mathbf{r}')} & & & \\ & \frac{\partial^2 u(\mathbf{r}_g,\mathbf{r}_s,\omega)}{\partial c_{44}(\mathbf{r})\partial c_{44}(\mathbf{r}')} & & \\ & & \frac{\partial^2 u(\mathbf{r}_g,\mathbf{r}_s,\omega)}{\partial c_{11}(\mathbf{r})\partial c_{11}(\mathbf{r}')} & \\ & & & \frac{\partial^2 u(\mathbf{r}_g,\mathbf{r}_s,\omega)}{\partial c_{13}(\mathbf{r})\partial c_{13}(\mathbf{r}')} \end{bmatrix}$$

The Diagonal Blocks

Multi-parameter Update and Multi-parameter Hessian within Gauss-Newton Framework

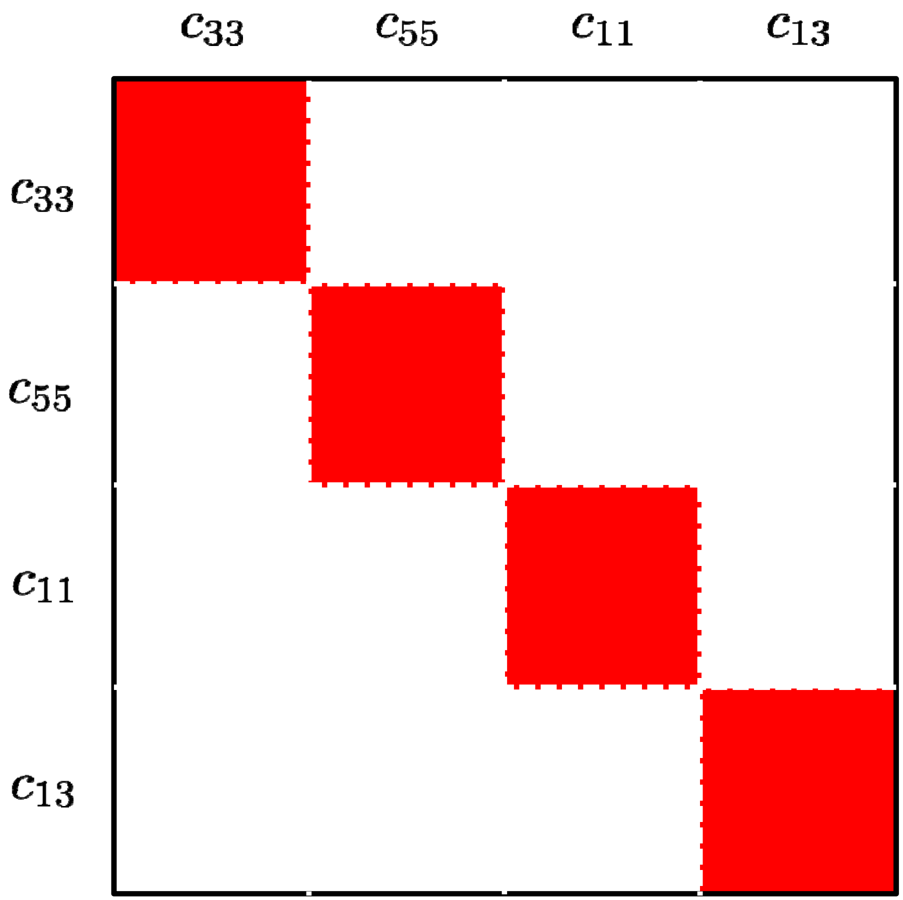

Schematic Diagram of the Diagonal Blocks

Multi-parameter Update and Multi-parameter Hessian within Gauss-Newton Framework

$$
\tilde{\mathbf{H}}_a(\mathbf{r},\mathbf{r}') = \begin{bmatrix}
 & \frac{\partial^2 u(\mathbf{r}_g,\mathbf{r}_s,\omega)}{\partial c_{33}(\mathbf{r}) c_{55}(\mathbf{r}')} & \frac{\partial^2 u(\mathbf{r}_g,\mathbf{r}_s,\omega)}{\partial c_{33}(\mathbf{r})\partial c_{11}(\mathbf{r}')} & \frac{\partial^2 u(\mathbf{r}_g,\mathbf{r}_s,\omega)}{\partial c_{33}(\mathbf{r})\partial c_{11}(\mathbf{r}')} \\
\frac{\partial^2 u(\mathbf{r}_g,\mathbf{r}_s,\omega)}{\partial c_{55}(\mathbf{r})\partial c_{33}(\mathbf{r}')} & & \frac{\partial^2 u(\mathbf{r}_g,\mathbf{r}_s,\omega)}{\partial c_{55}(\mathbf{r})\partial c_{11}(\mathbf{r}')} & \frac{\partial^2 u(\mathbf{r}_g,\mathbf{r}_s,\omega)}{\partial c_{55}(\mathbf{r})\partial c_{13}(\mathbf{r}')} \\
\frac{\partial^2 u(\mathbf{r}_g,\mathbf{r}_s,\omega)}{\partial c_{11}(\mathbf{r})\partial c_{33}(\mathbf{r}')} & \frac{\partial^2 u(\mathbf{r}_g,\mathbf{r}_s,\omega)}{\partial c_{11}(\mathbf{r})\partial c_{55}(\mathbf{r}')} & & \frac{\partial^2 u(\mathbf{r}_g,\mathbf{r}_s,\omega)}{\partial c_{11}(\mathbf{r})\partial c_{13}(\mathbf{r}')} \\
\frac{\partial^2 u(\mathbf{r}_g,\mathbf{r}_s,\omega)}{\partial c_{13}(\mathbf{r})\partial c_{33}(\mathbf{r}')} & \frac{\partial^2 u(\mathbf{r}_g,\mathbf{r}_s,\omega)}{\partial c_{13}(\mathbf{r})\partial c_{55}(\mathbf{r}')} & \frac{\partial^2 u(\mathbf{r}_g,\mathbf{r}_s,\omega)}{\partial c_{13}(\mathbf{r})\partial c_{11}(\mathbf{r}')} &
\end{bmatrix}
$$

Off-diagonal Blocks of the Multi-parameter Hessian Control Cross-talk

Multi-parameter Update and Multi-parameter Hessian within Gauss-Newton Framework

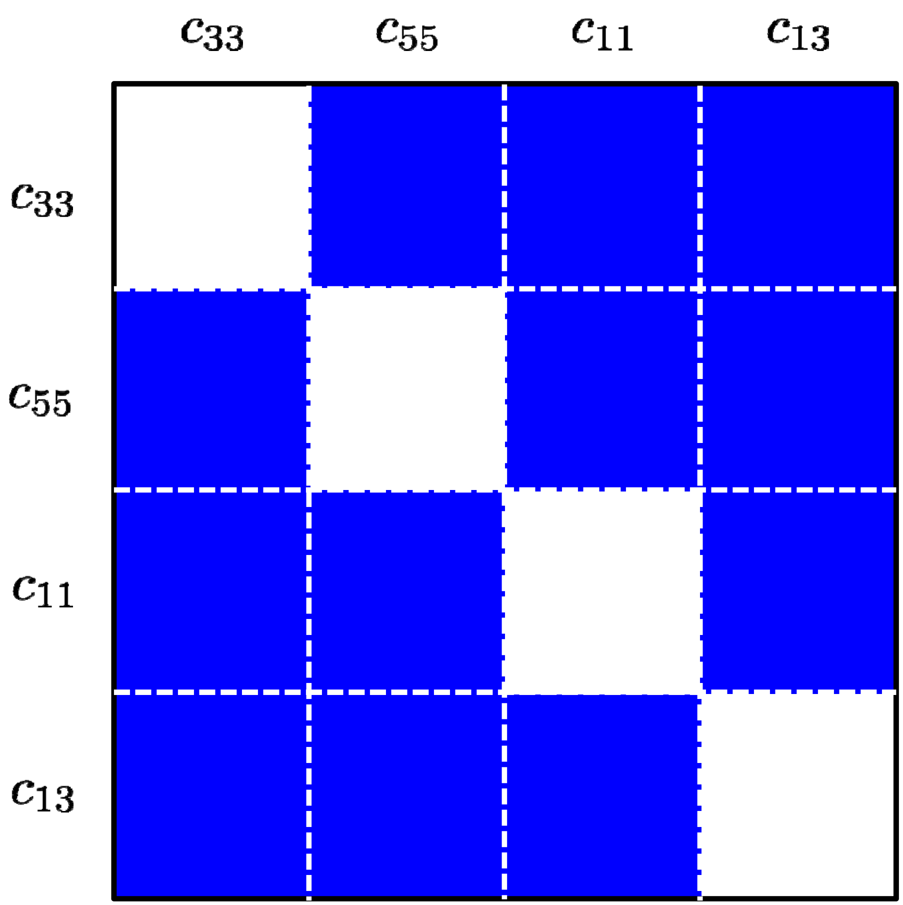

Schematic Diagram of the Off-diagonal Blocks

Multi-parameter Update and Multi-parameter Hessian within Gauss-Newton Framework

$$\hat{\mathbf{H}}_a(\mathbf{r}) = \begin{bmatrix} & \frac{\partial^2 u(\mathbf{r}_g,\mathbf{r}_s,\omega)}{\partial c_{33}(\mathbf{r})\partial c_{55}(\mathbf{r})} & \frac{\partial^2 u(\mathbf{r}_g,\mathbf{r}_s,\omega)}{\partial c_{33}(\mathbf{r})\partial c_{11}(\mathbf{r})} & \frac{\partial^2 u(\mathbf{r}_g,\mathbf{r}_s,\omega)}{\partial c_{33}(\mathbf{r})\partial c_{11}(\mathbf{r})} \\ \frac{\partial^2 u(\mathbf{r}_g,\mathbf{r}_s,\omega)}{\partial c_{55}(\mathbf{r})\partial c_{33}(\mathbf{r})} & & \frac{\partial^2 u(\mathbf{r}_g,\mathbf{r}_s,\omega)}{\partial c_{55}(\mathbf{r})\partial c_{11}(\mathbf{r})} & \frac{\partial^2 u(\mathbf{r}_g,\mathbf{r}_s,\omega)}{\partial c_{55}(\mathbf{r})\partial c_{13}(\mathbf{r})} \\ \frac{\partial^2 u(\mathbf{r}_g,\mathbf{r}_s,\omega)}{\partial c_{11}(\mathbf{r})\partial c_{33}(\mathbf{r})} & \frac{\partial^2 u(\mathbf{r}_g,\mathbf{r}_s,\omega)}{\partial c_{11}(\mathbf{r})\partial c_{55}(\mathbf{r})} & & \frac{\partial^2 u(\mathbf{r}_g,\mathbf{r}_s,\omega)}{\partial c_{11}(\mathbf{r})\partial c_{13}(\mathbf{r})} \\ \frac{\partial^2 u(\mathbf{r}_g,\mathbf{r}_s,\omega)}{\partial c_{13}(\mathbf{r})\partial c_{33}(\mathbf{r})} & \frac{\partial^2 u(\mathbf{r}_g,\mathbf{r}_s,\omega)}{\partial c_{13}(\mathbf{r})\partial c_{55}(\mathbf{r})} & \frac{\partial^2 u(\mathbf{r}_g,\mathbf{r}_s,\omega)}{\partial c_{13}(\mathbf{r})\partial c_{11}(\mathbf{r})} & \end{bmatrix}$$

The Parameter-type Approximation (Innanen, 2014)

Multi-parameter Update and Multi-parameter Hessian within Gauss-Newton Framework

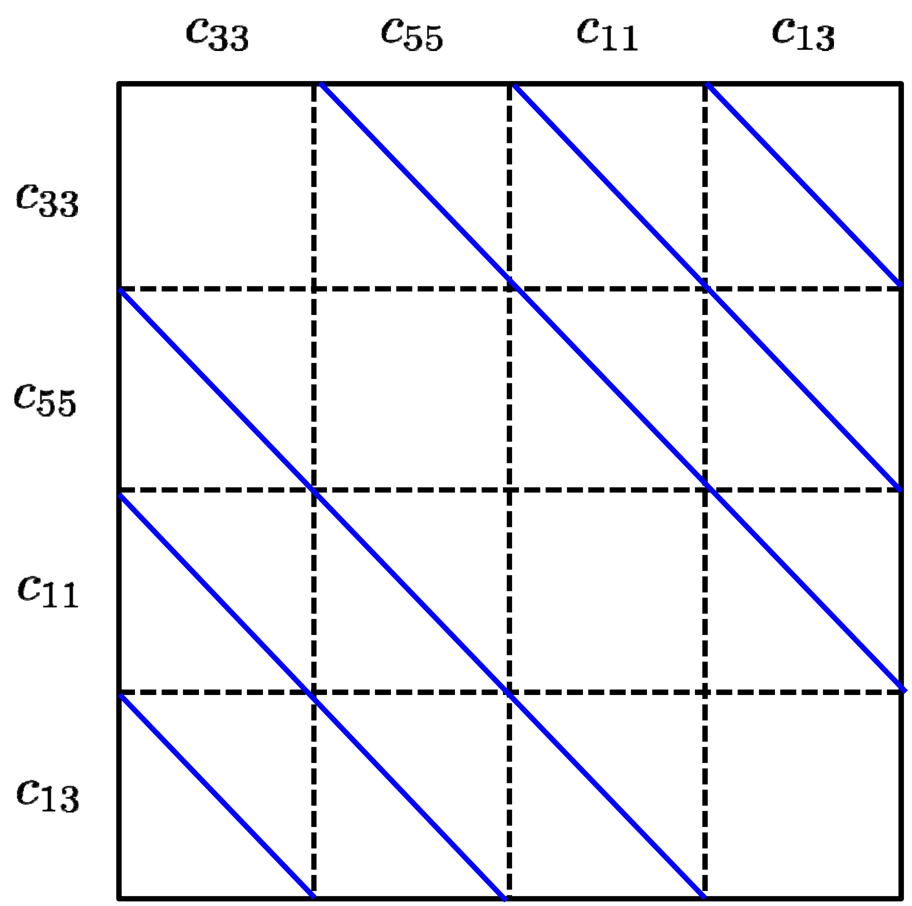

Schematic Diagram of the Parameter-type Approximation

Numerical Experiments

1. Inversion Sensitivity Analysis: Analytic Results vs. Numerical Modelling Results

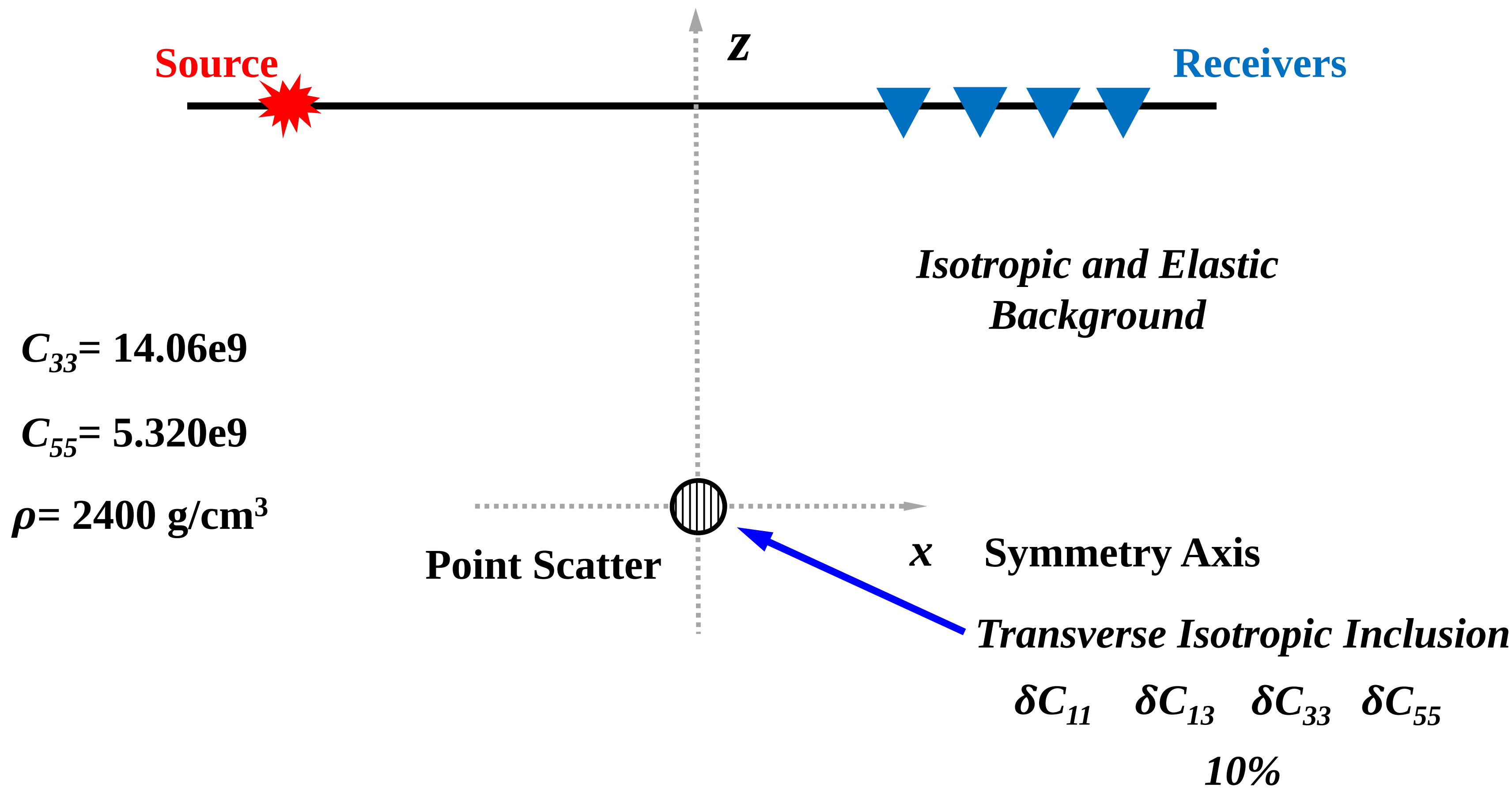

Source
z
Receivers
Isotropic and Elastic
Background
C_{33}= 14.06e9
C_{55}= 5.320e9
ρ= 2400 g/cm^3
Point Scatter
x
Symmetry Axis
Transverse Isotropic Inclusion
δC_{11} δC_{13} δC_{33} δC_{55}
10%

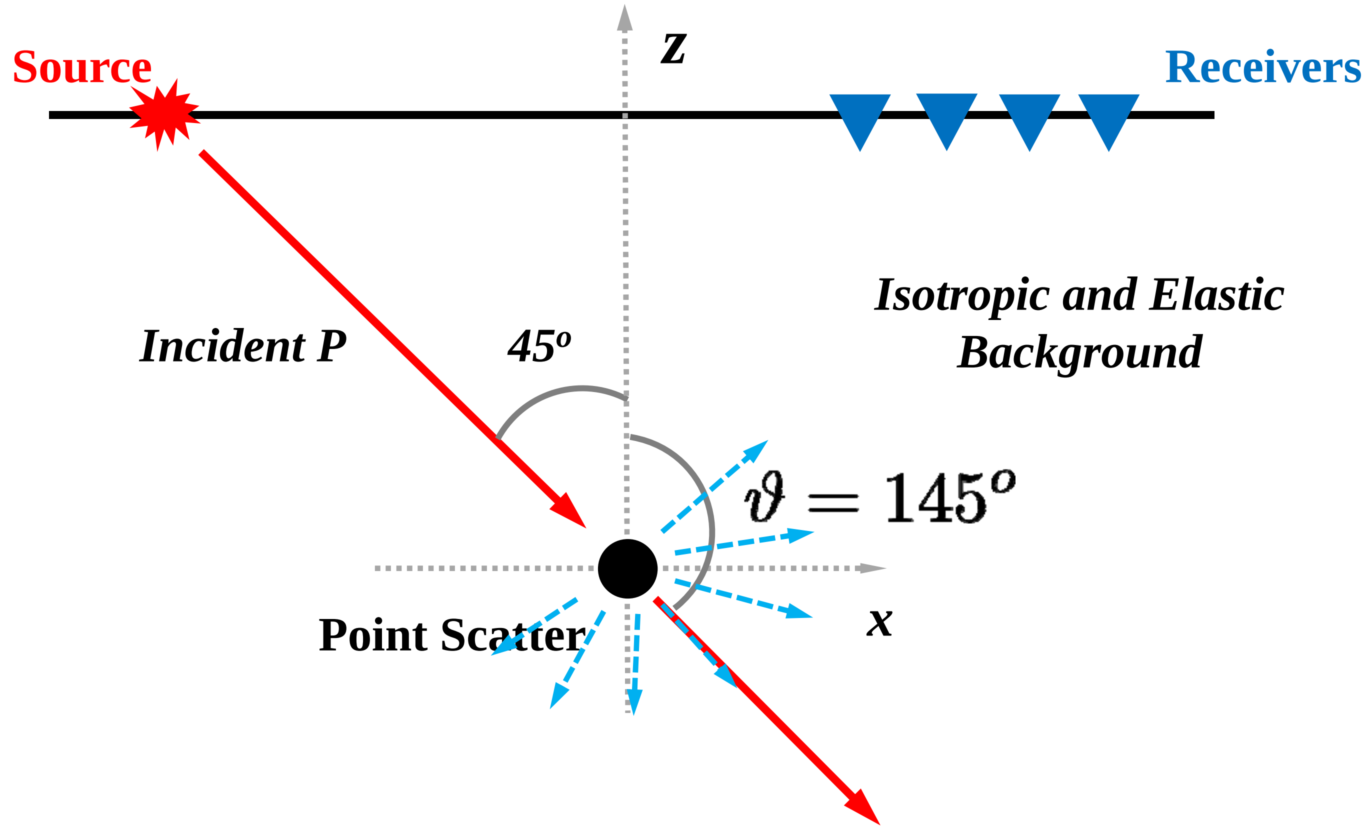

Incident P Wave $\vartheta = 145^o, \varphi = 0^o$

$$\frac{\partial u}{\partial m}, m \in (c_{33}, c_{55}, c_{11}, c_{13})$$

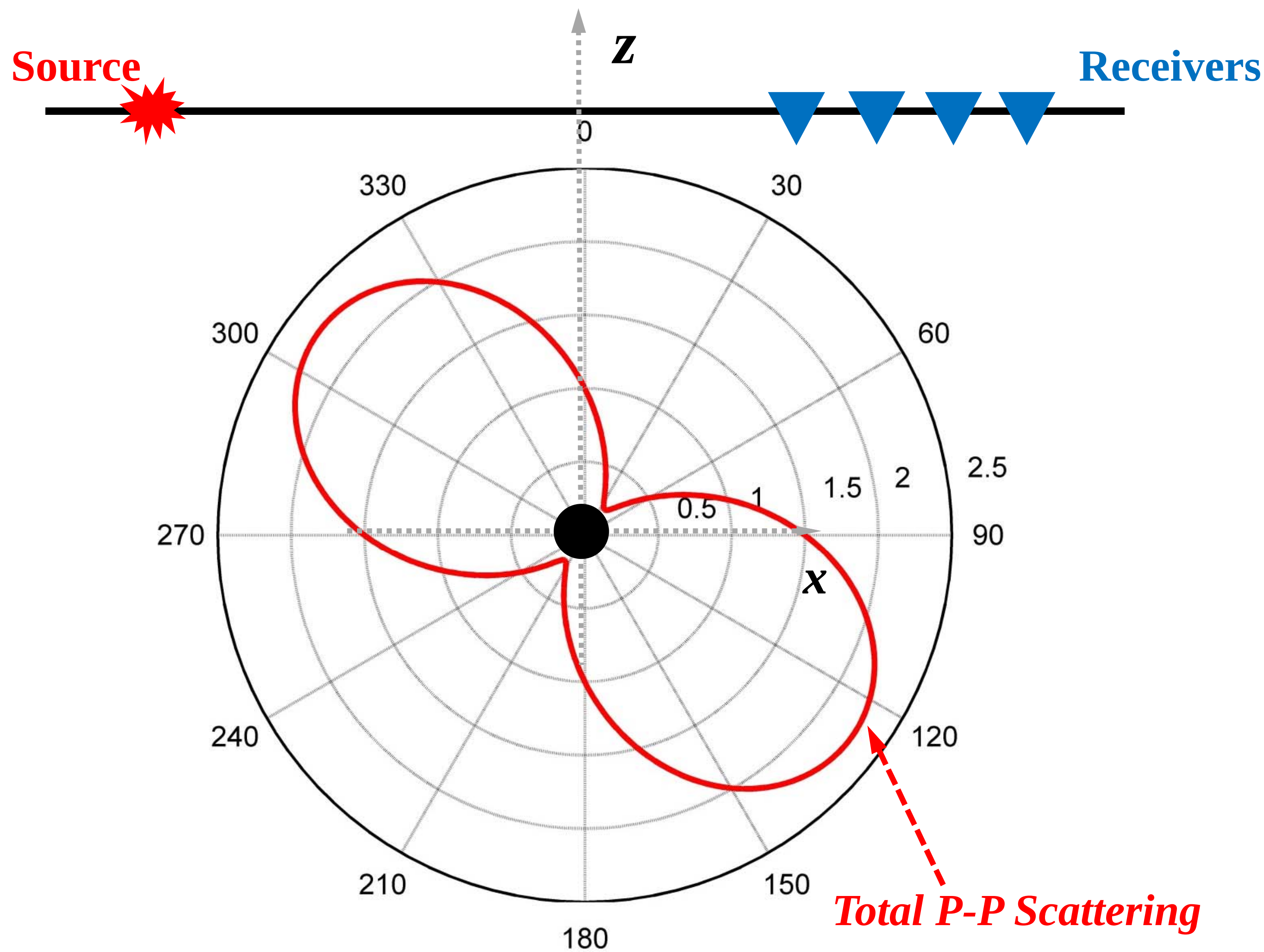

$$\frac{\partial u}{\partial m}, m \in (c_{33}, c_{55}, c_{11}, c_{13})$$

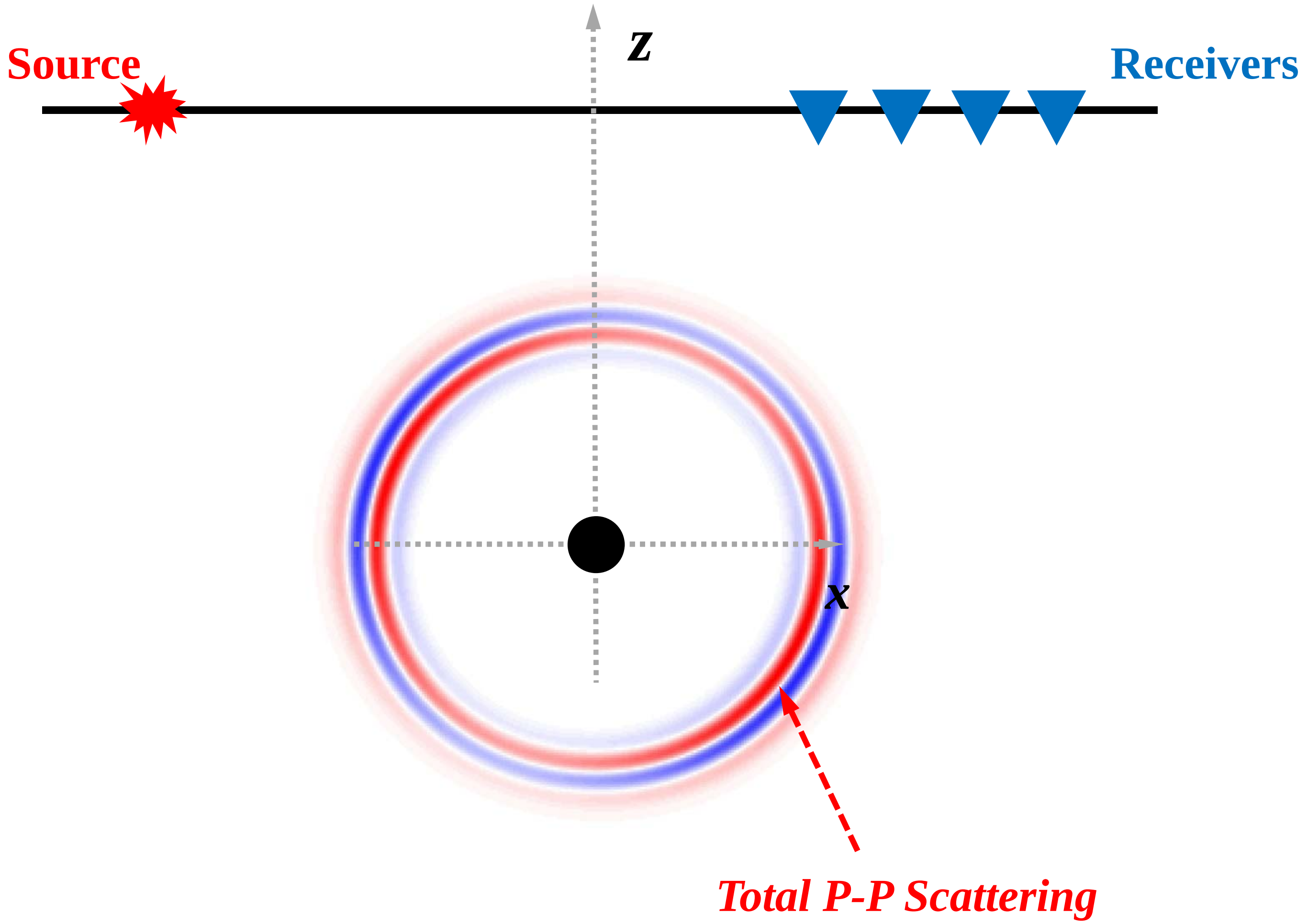

$$\frac{\partial u}{\partial c_{33}}$$

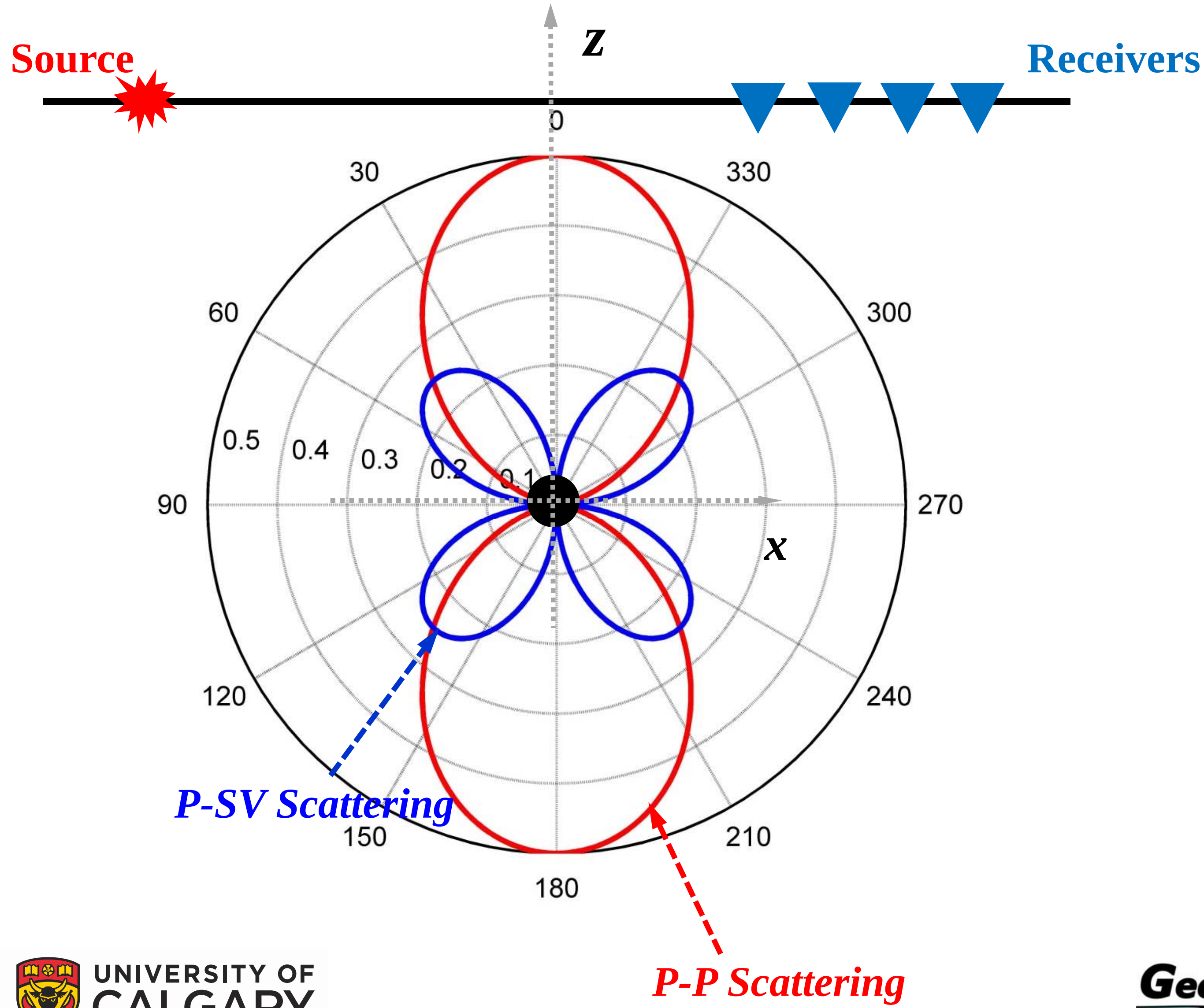

$$\frac{\partial u}{\partial c_{33}}$$

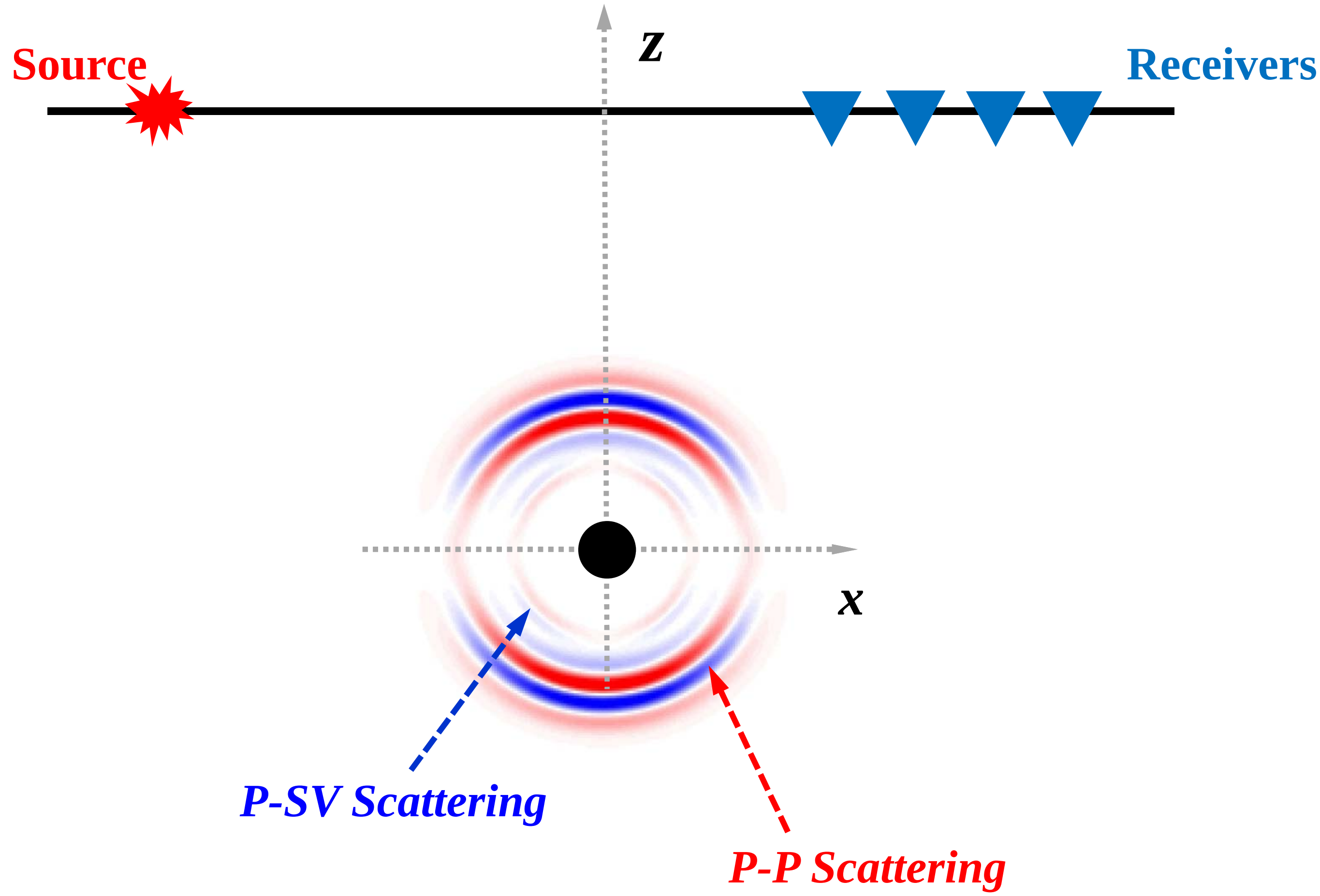

$$\frac{\partial u}{\partial c_{55}}$$

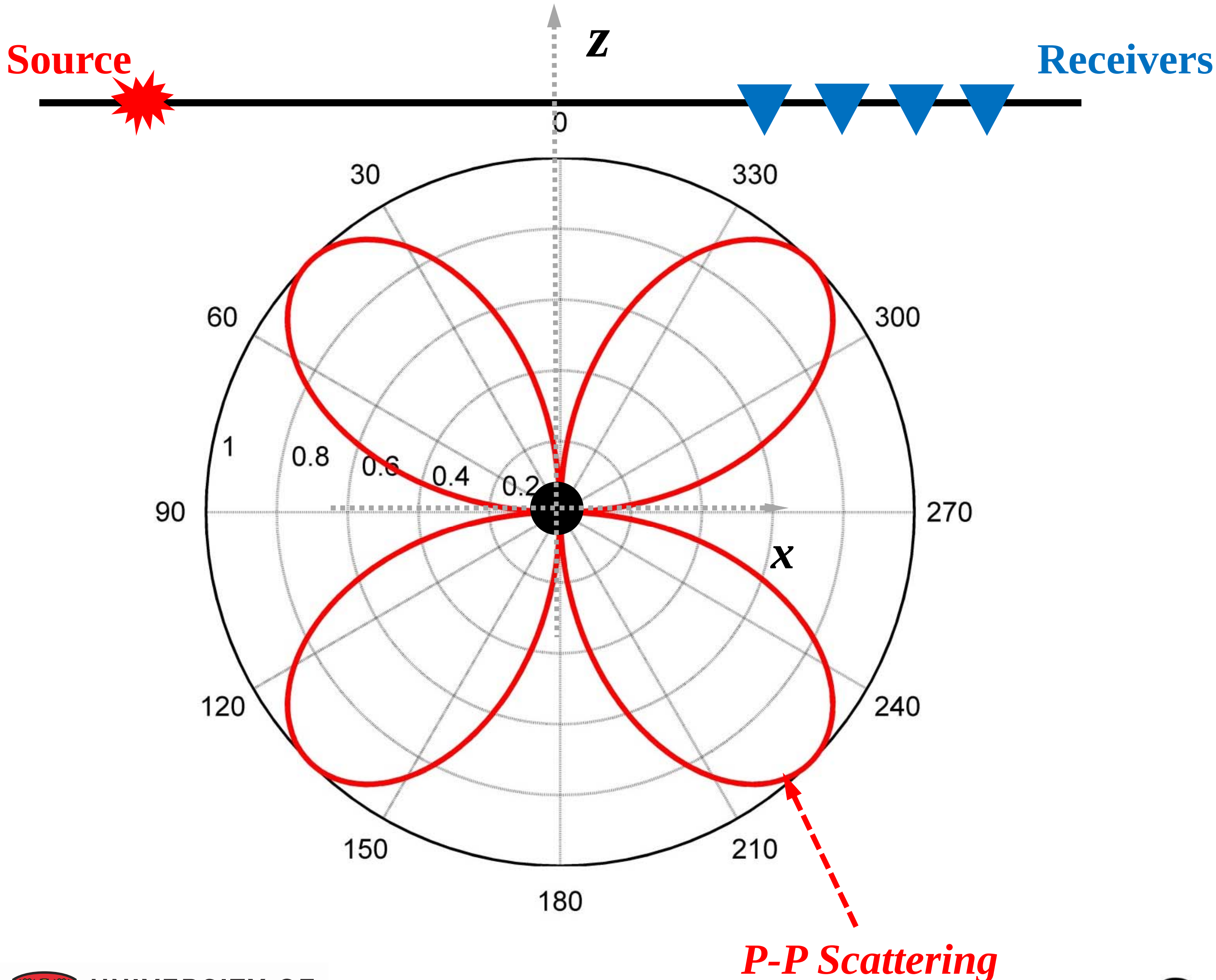

$$\frac{\partial u}{\partial c_{55}}$$

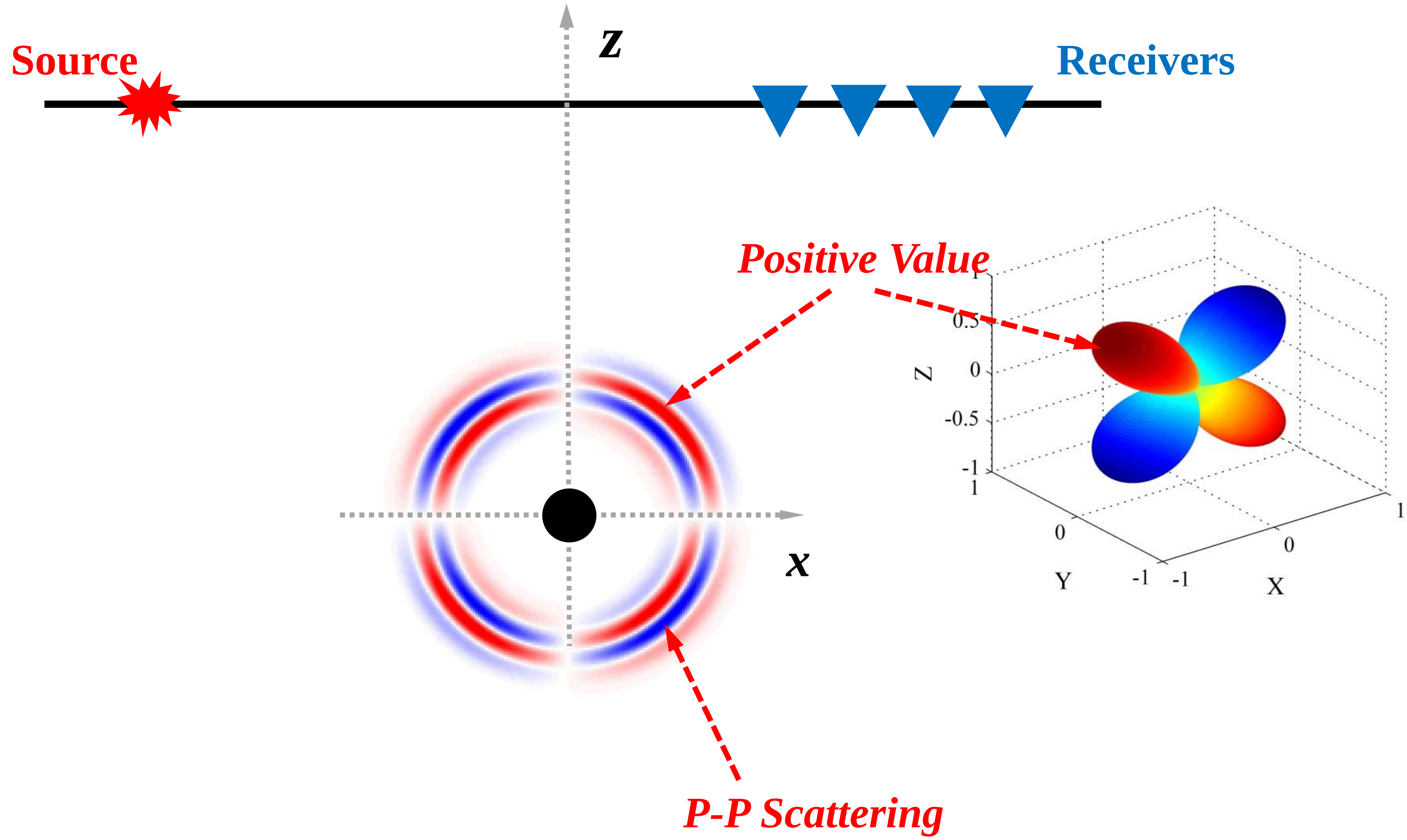

$$\frac{\partial u}{\partial c_{11}}$$

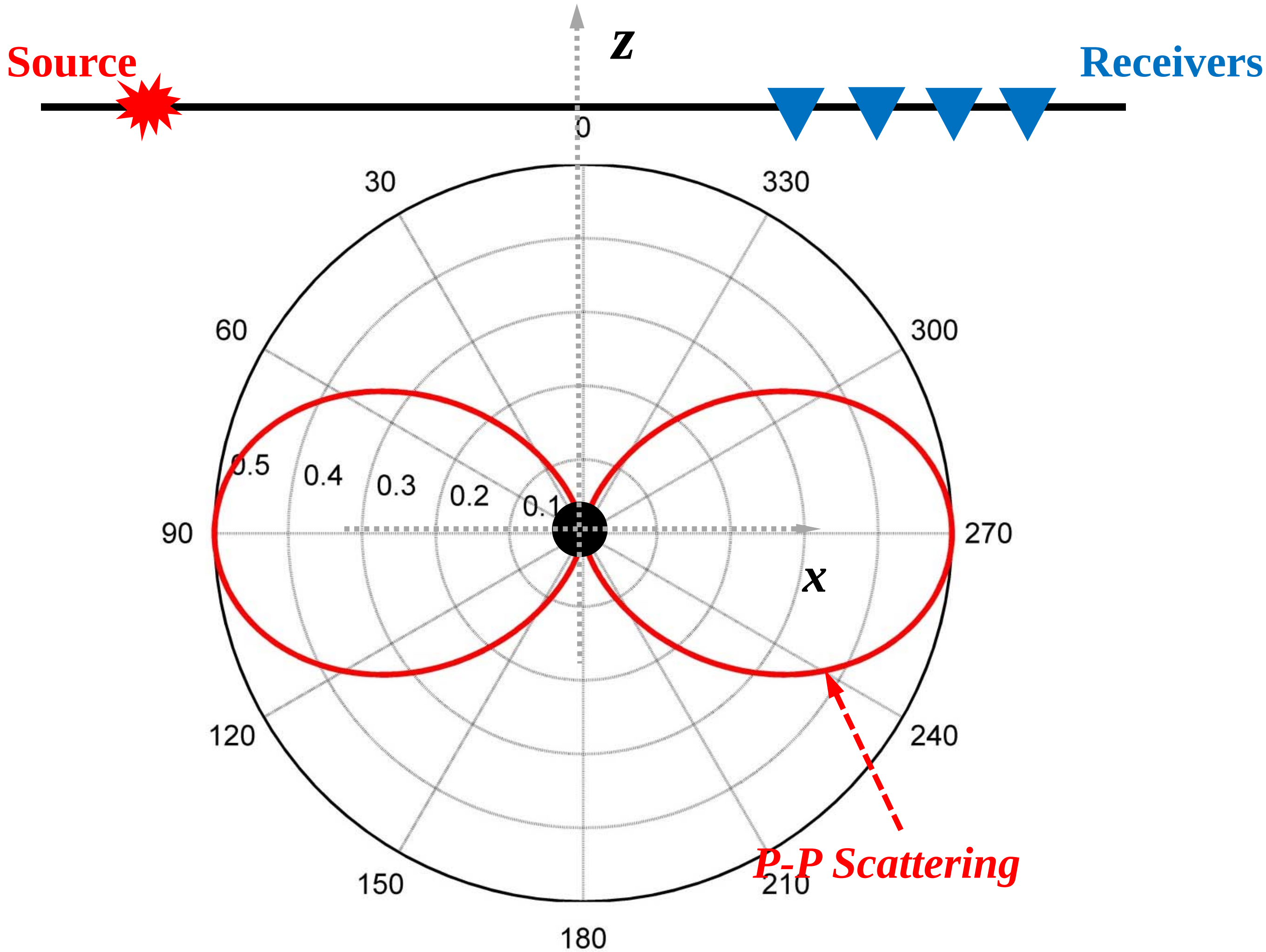

$$\frac{\partial u}{\partial c_{11}}$$

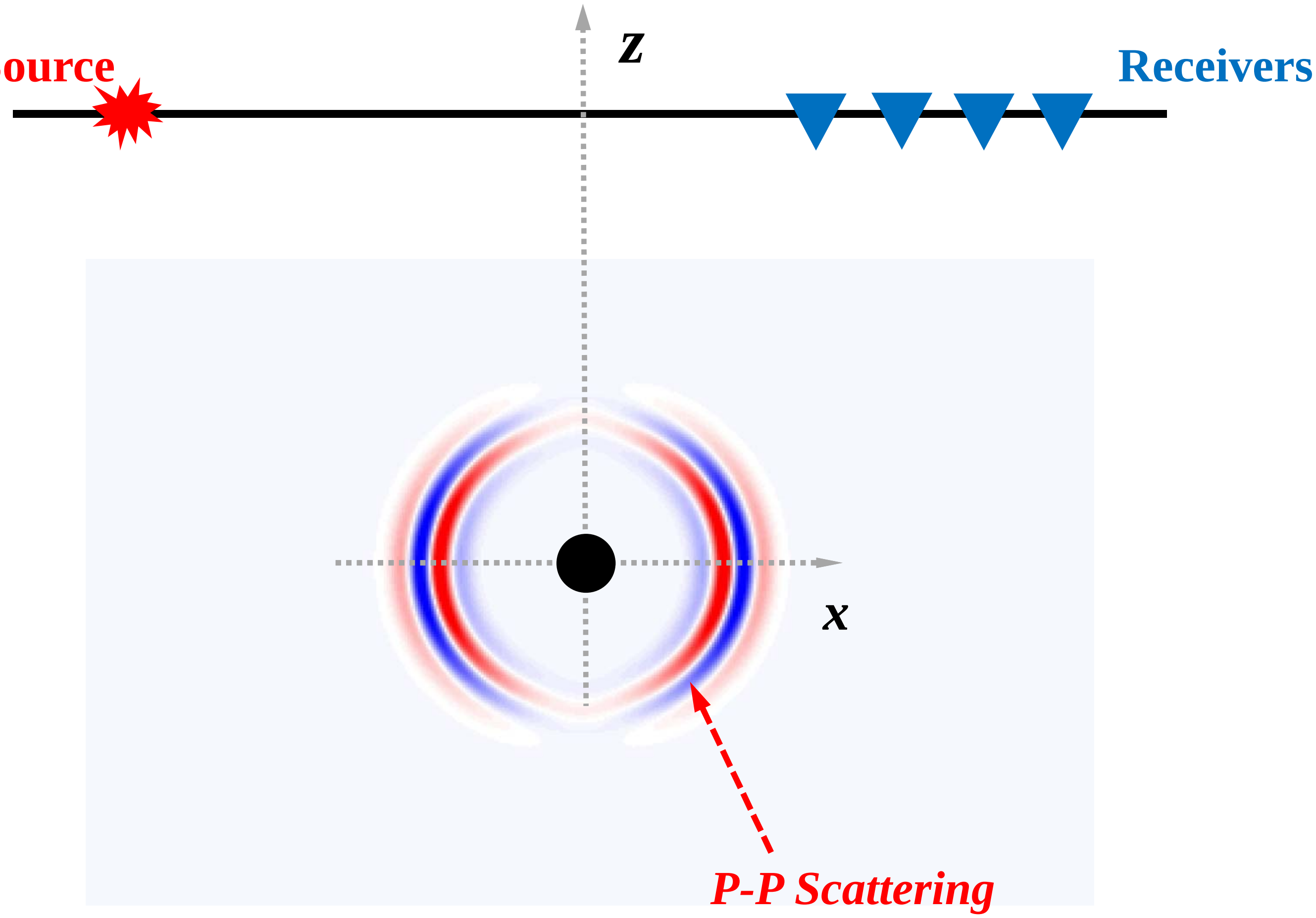

$$\frac{\partial u}{\partial c_{13}}$$

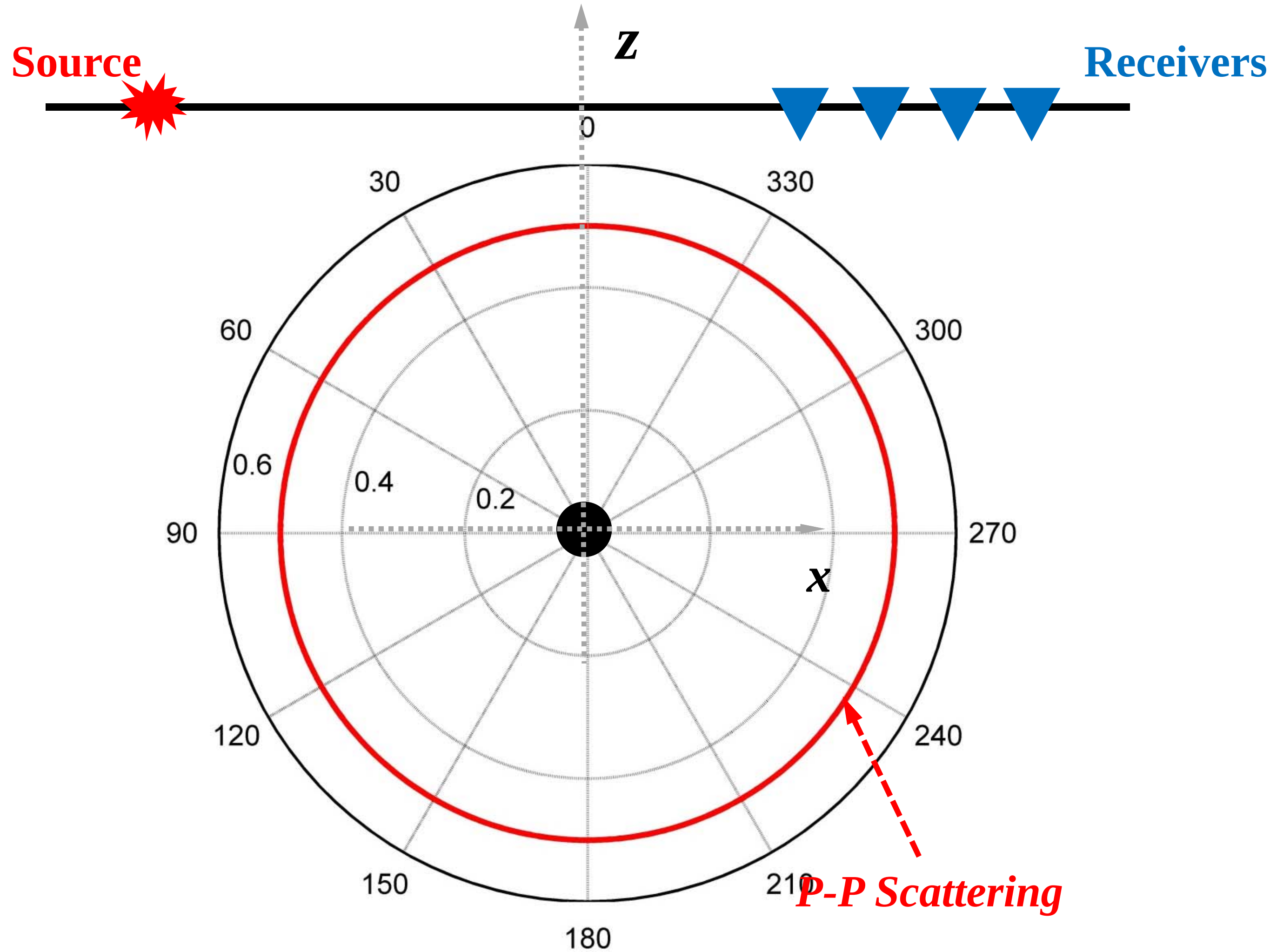

$$\frac{\partial u}{\partial c_{13}}$$

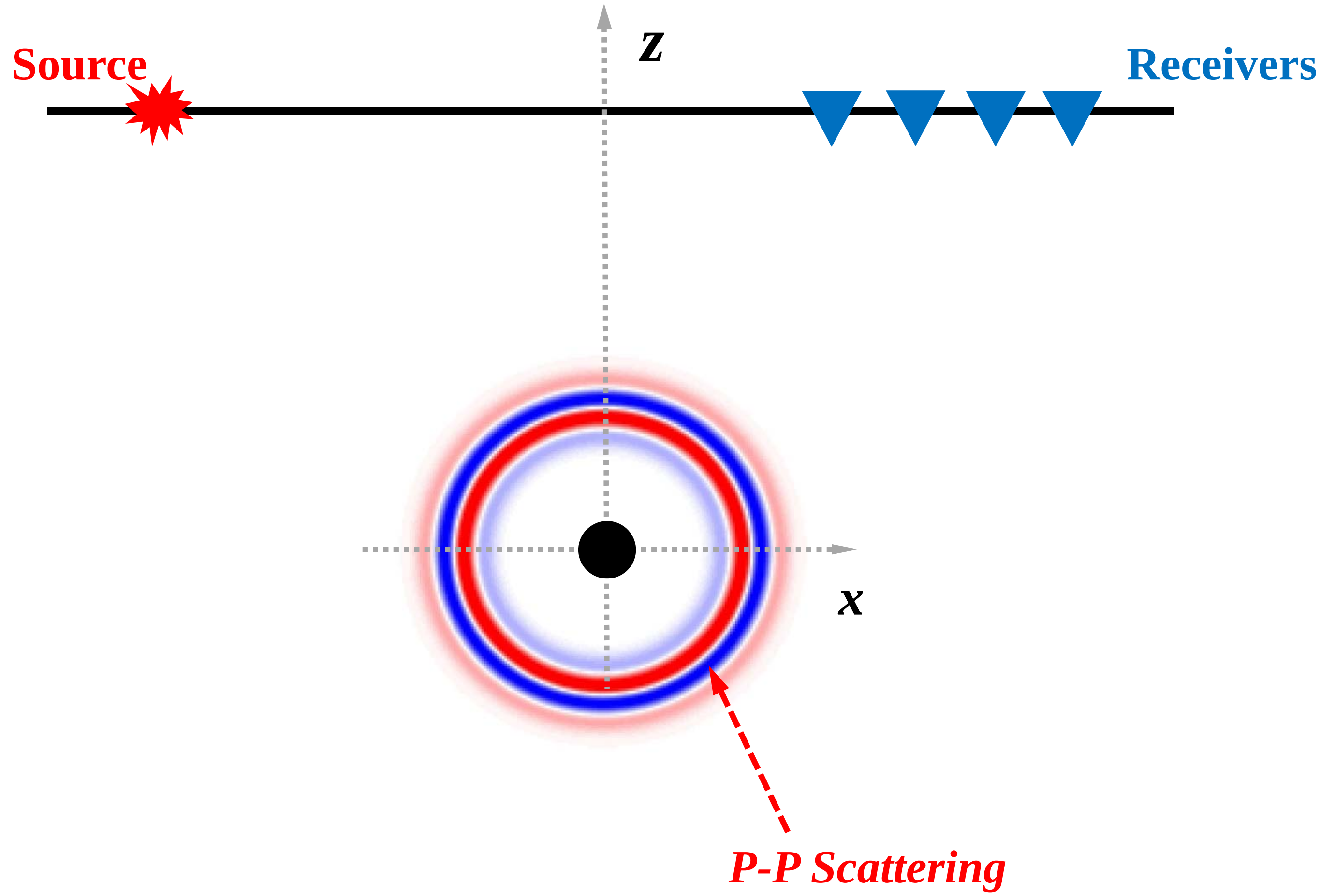

2. Elastic Constants Estimation Using a 2D HTI Model

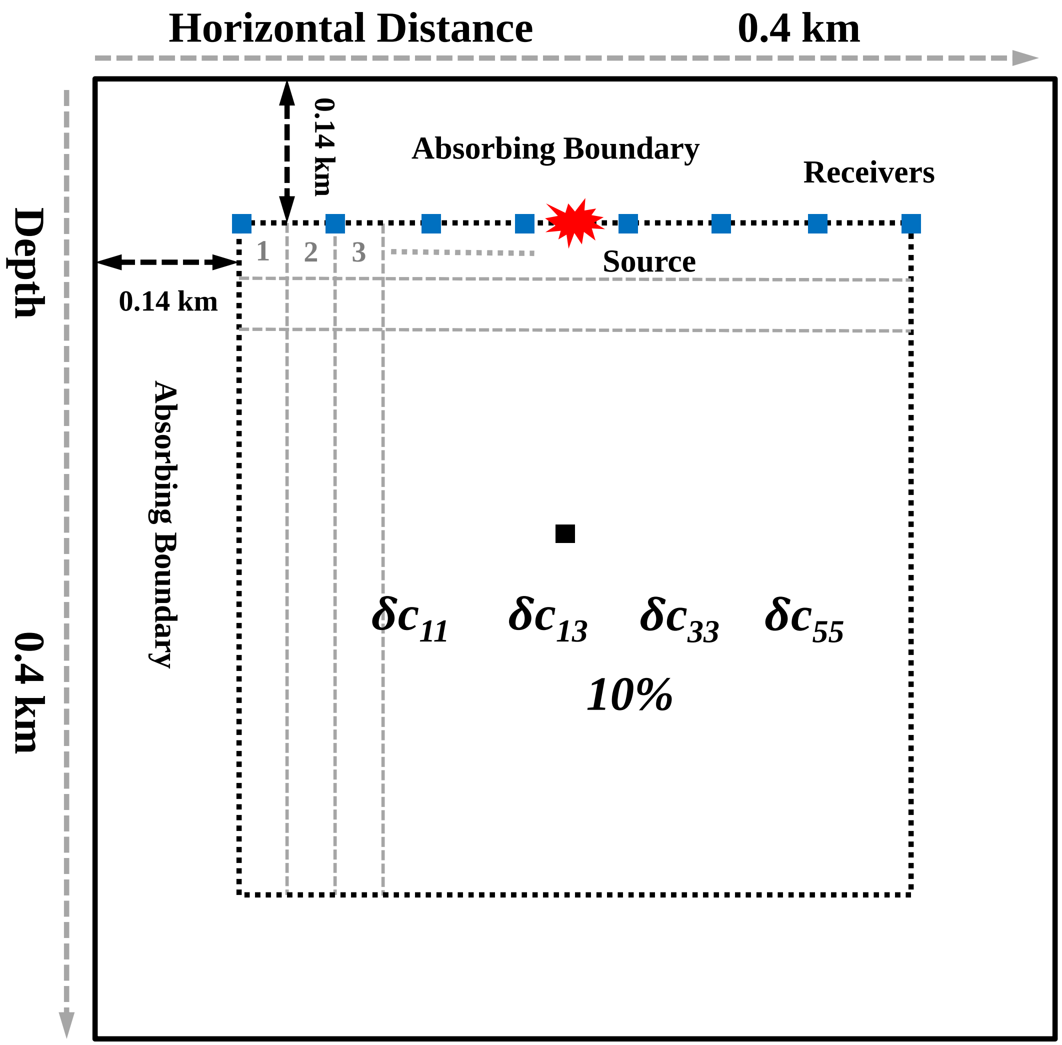

Isotropic Background

c_{11}= 14.06 GPa

c_{55}= 6.320 GPa

ρ= 2.4 kg/m^3

v_p=2420 m/s

v_s= 1623 m/s

ρ= 2.4 kg/m^3

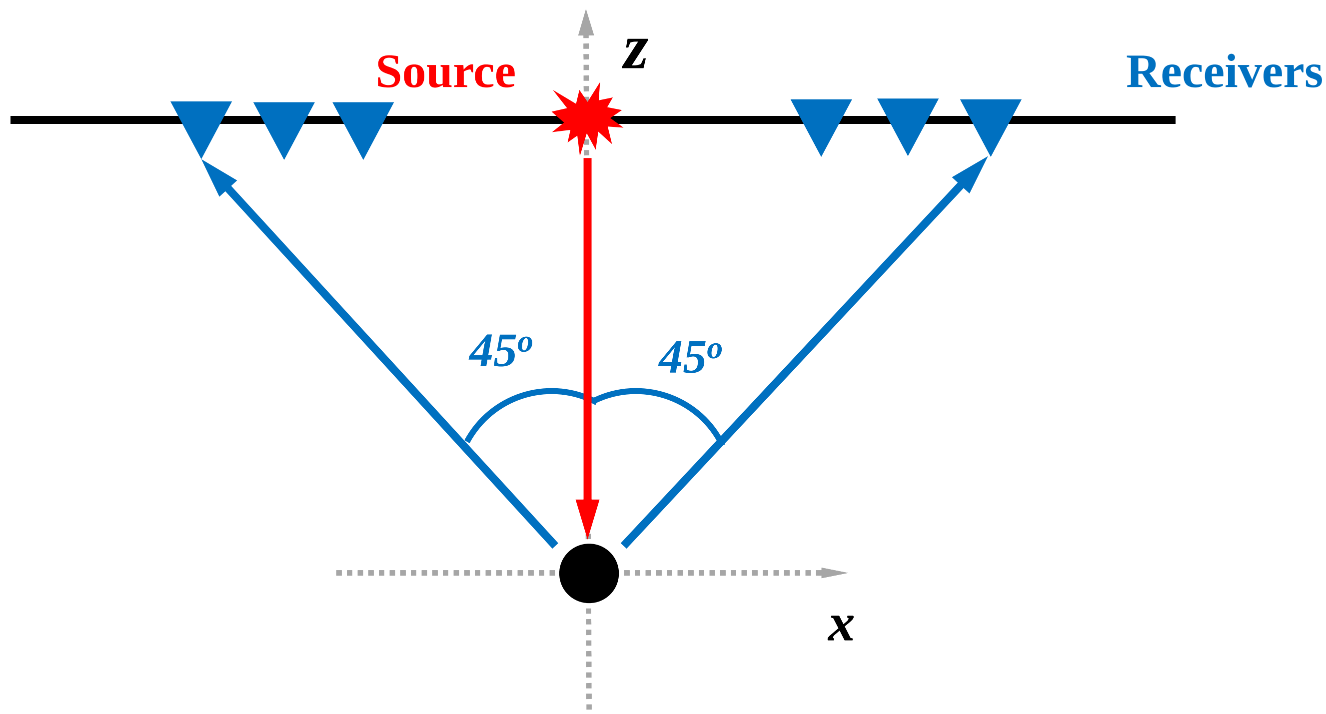

δc_{11} δc_{13} δc_{33} δc_{55}

10%

Incident Wave $\vartheta = 180^o, \varphi = 0^o$

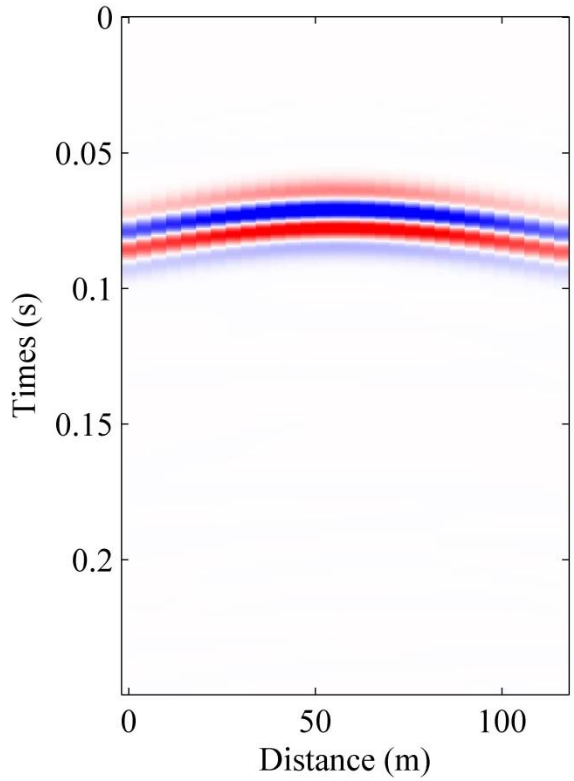

Total data residuals δc_{33} δc_{55} δc_{11} δc_{13}

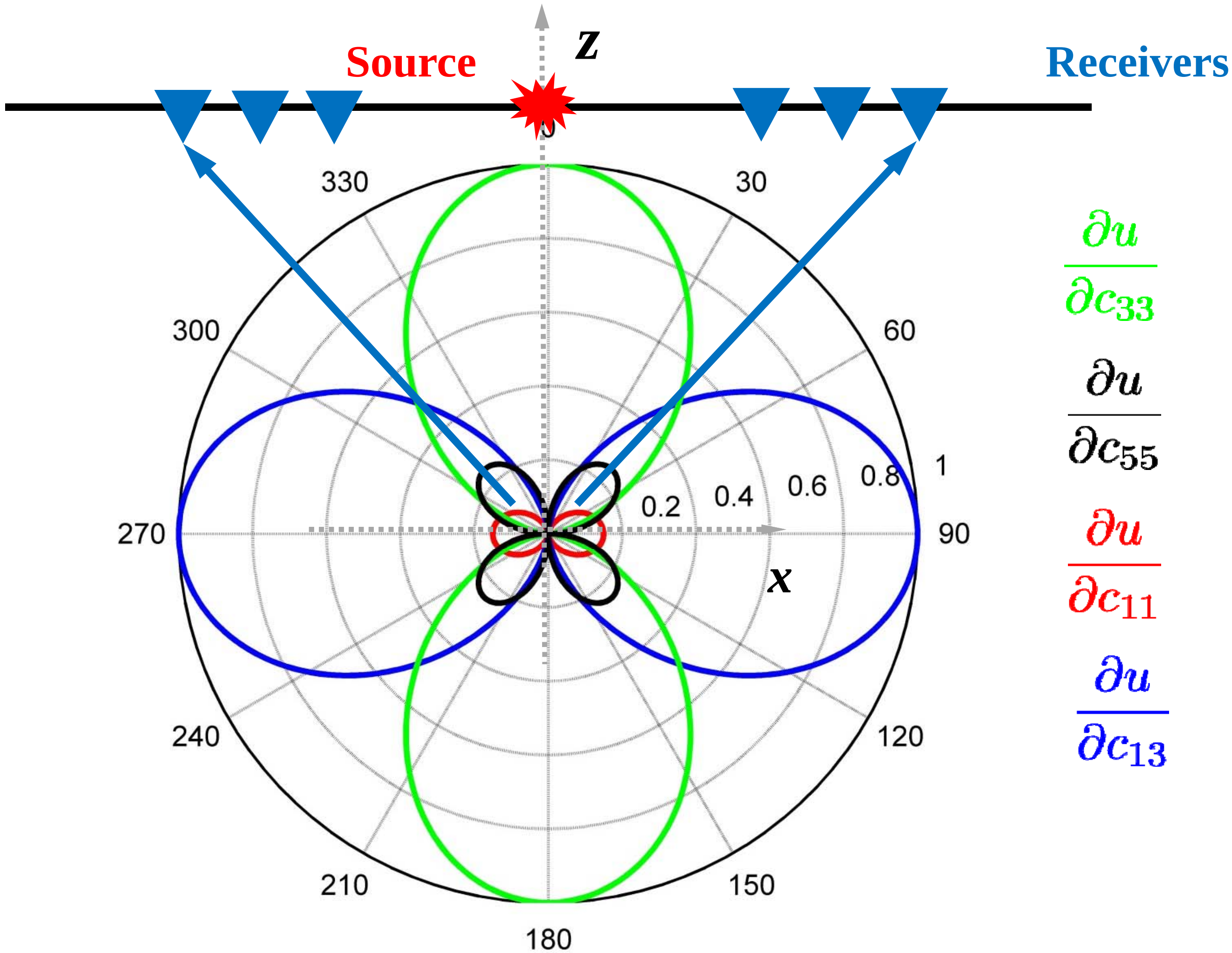

P-P Scattering Patterns

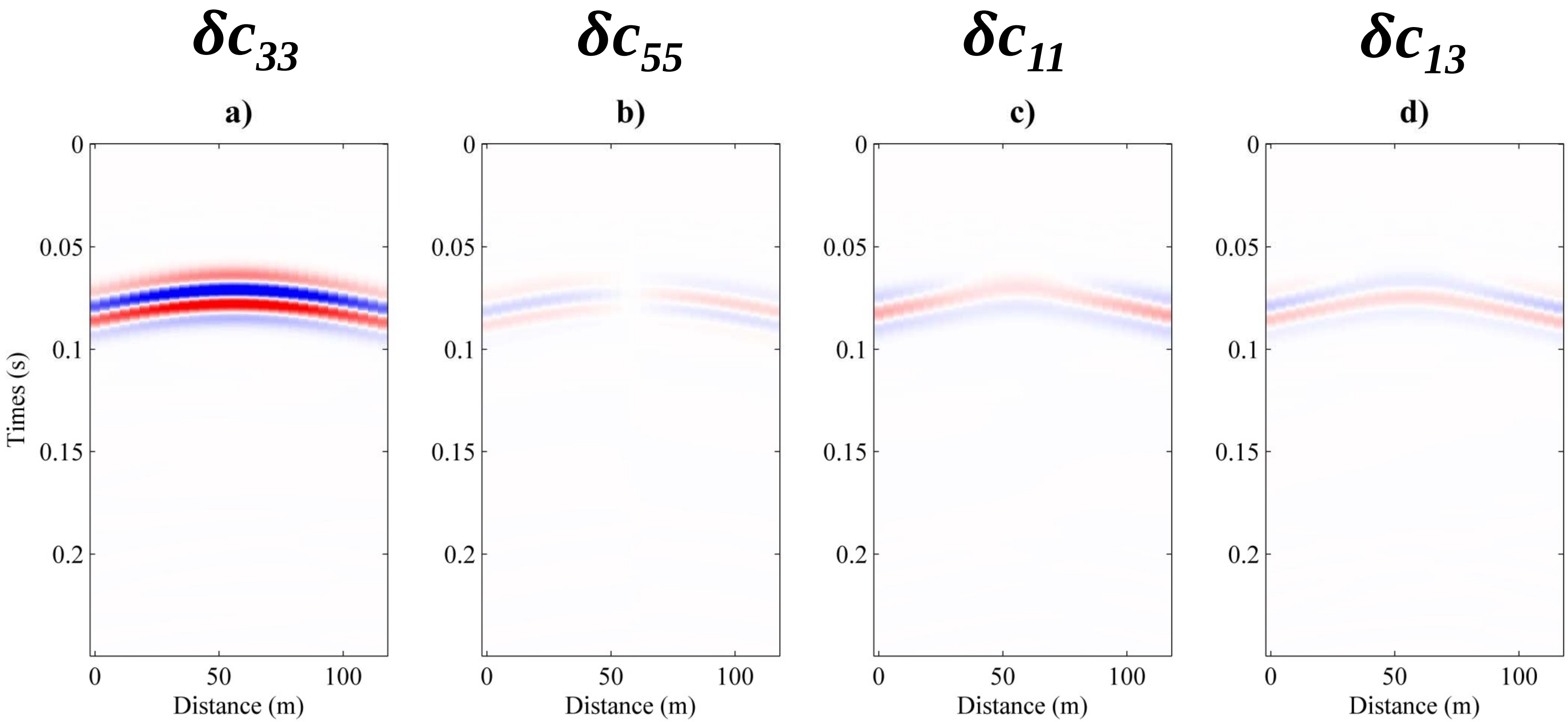

Data residuals by different parameters

$$\frac{\partial^2 u}{\partial v_p^2}$$

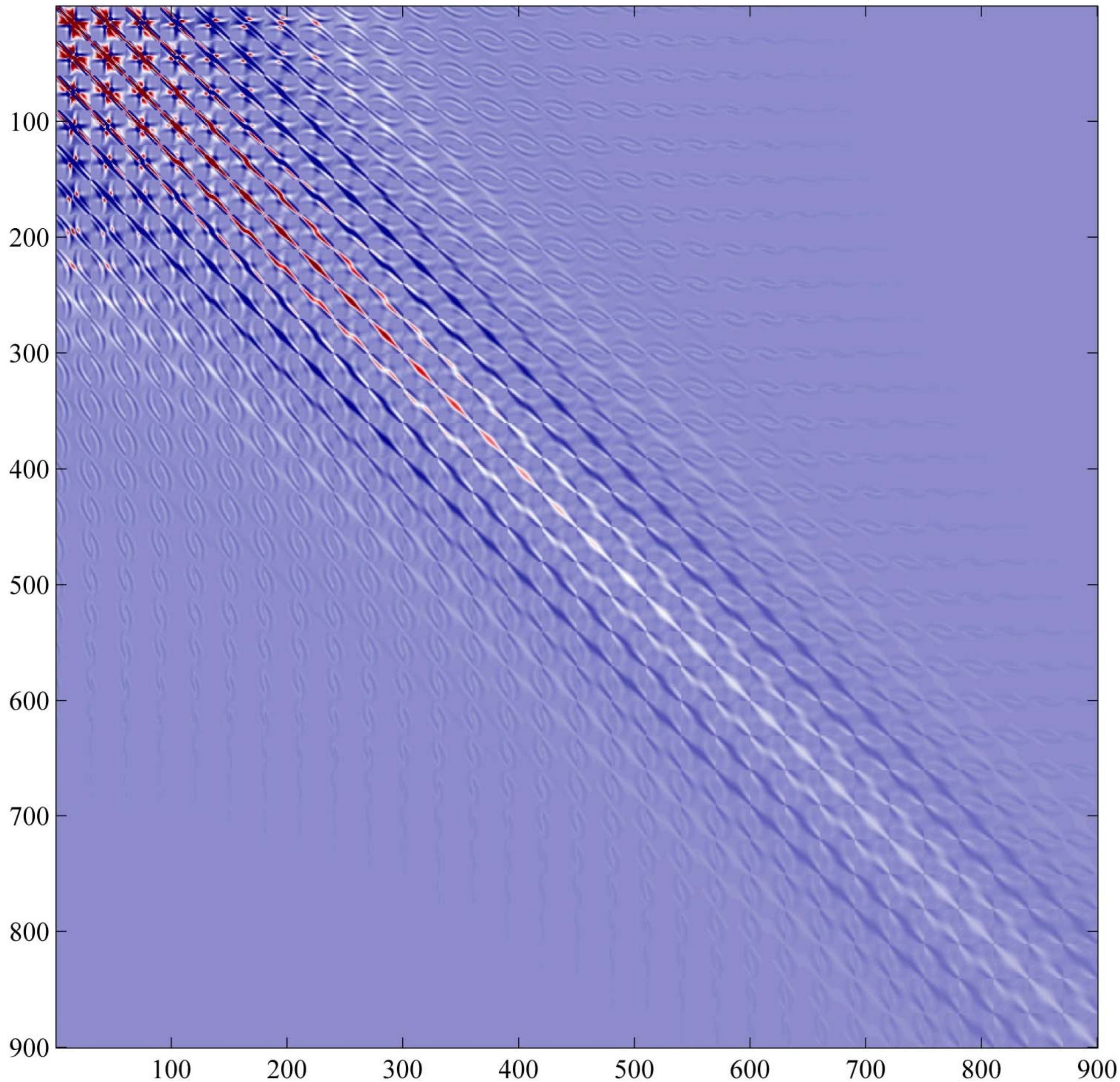

	c_{33}	c_{55}	c_{11}	c_{13}
c_{33}	$\frac{\partial^2 u}{\partial c_{33}^2}$	$\frac{\partial^2 u}{\partial c_{33} \partial c_{55}}$	$\frac{\partial^2 u}{\partial c_{33} \partial c_{11}}$	$\frac{\partial^2 u}{\partial c_{33} \partial c_{13}}$
c_{55}	$\frac{\partial^2 u}{\partial c_{33} \partial c_{55}}$	$\frac{\partial^2 u}{\partial c_{55}^2}$	$\frac{\partial^2 u}{\partial c_{55} \partial c_{11}}$	$\frac{\partial^2 u}{\partial c_{55} \partial c_{13}}$
c_{11}	$\frac{\partial^2 u}{\partial c_{33} \partial c_{11}}$	$\frac{\partial^2 u}{\partial c_{55} \partial c_{11}}$	$\frac{\partial^2 u}{\partial c_{11}^2}$	$\frac{\partial^2 u}{\partial c_{11} \partial c_{13}}$
c_{13}	$\frac{\partial^2 u}{\partial c_{33} \partial c_{11}}$	$\frac{\partial^2 u}{\partial c_{55} \partial c_{13}}$	$\frac{\partial^2 u}{\partial c_{11} \partial c_{13}}$	$\frac{\partial^2 u}{\partial c_{13}^2}$

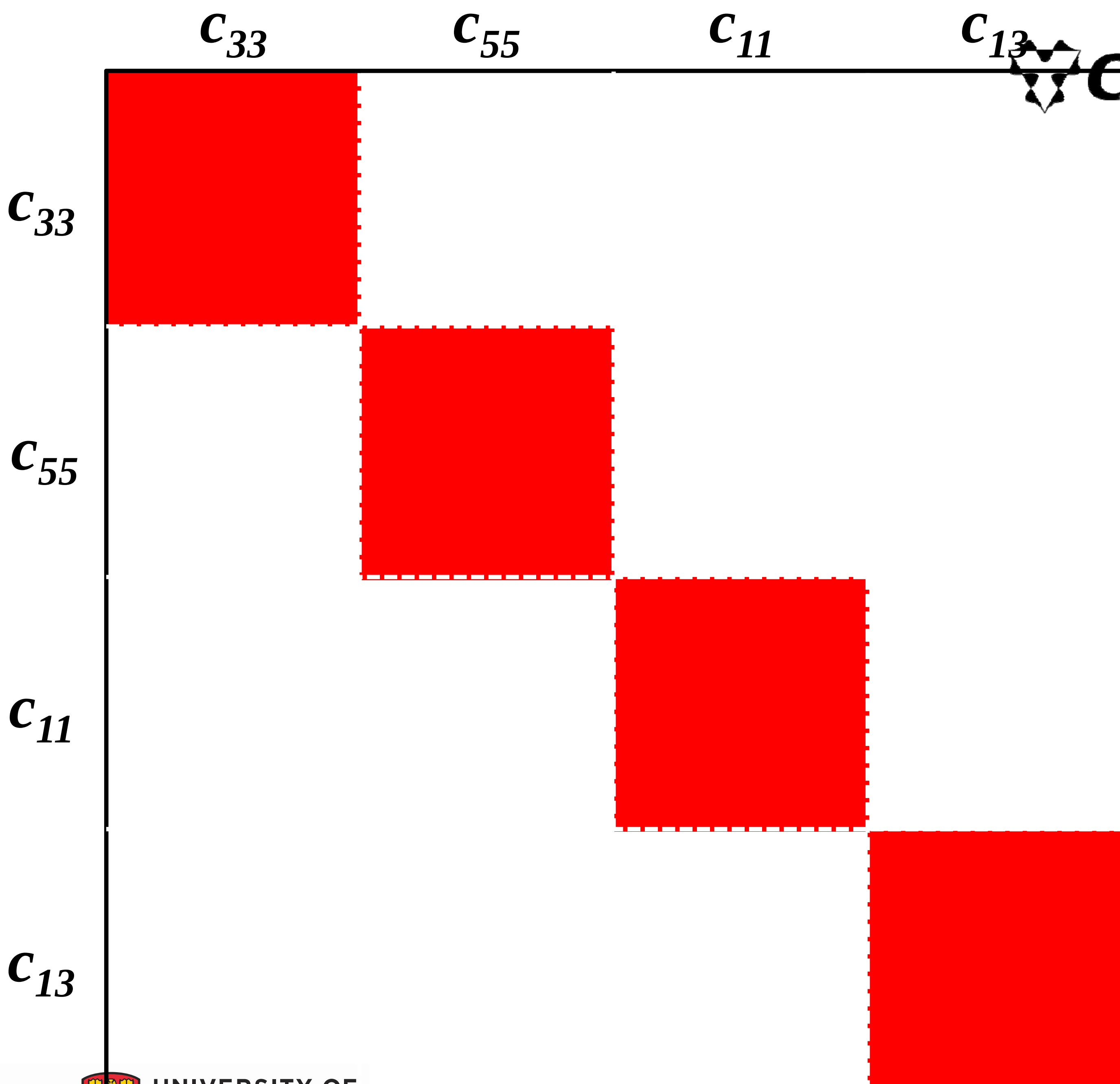

Space-type Approximation

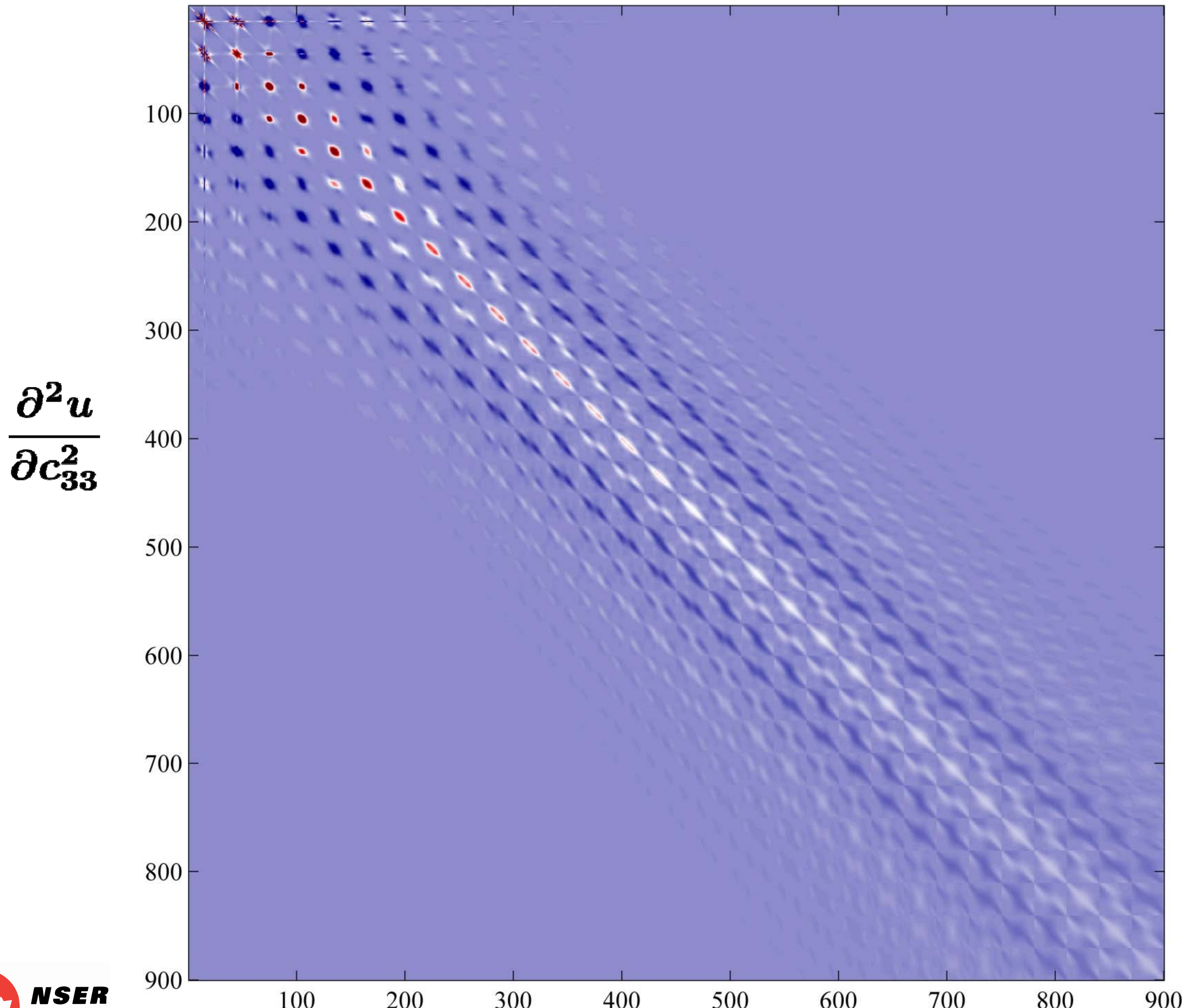

$\frac{\partial^2 u}{\partial c_{33}^2}$
100
200
300
400
500
600
700
800
900

$$\frac{\partial^2 u}{\partial c_{55}^2}$$

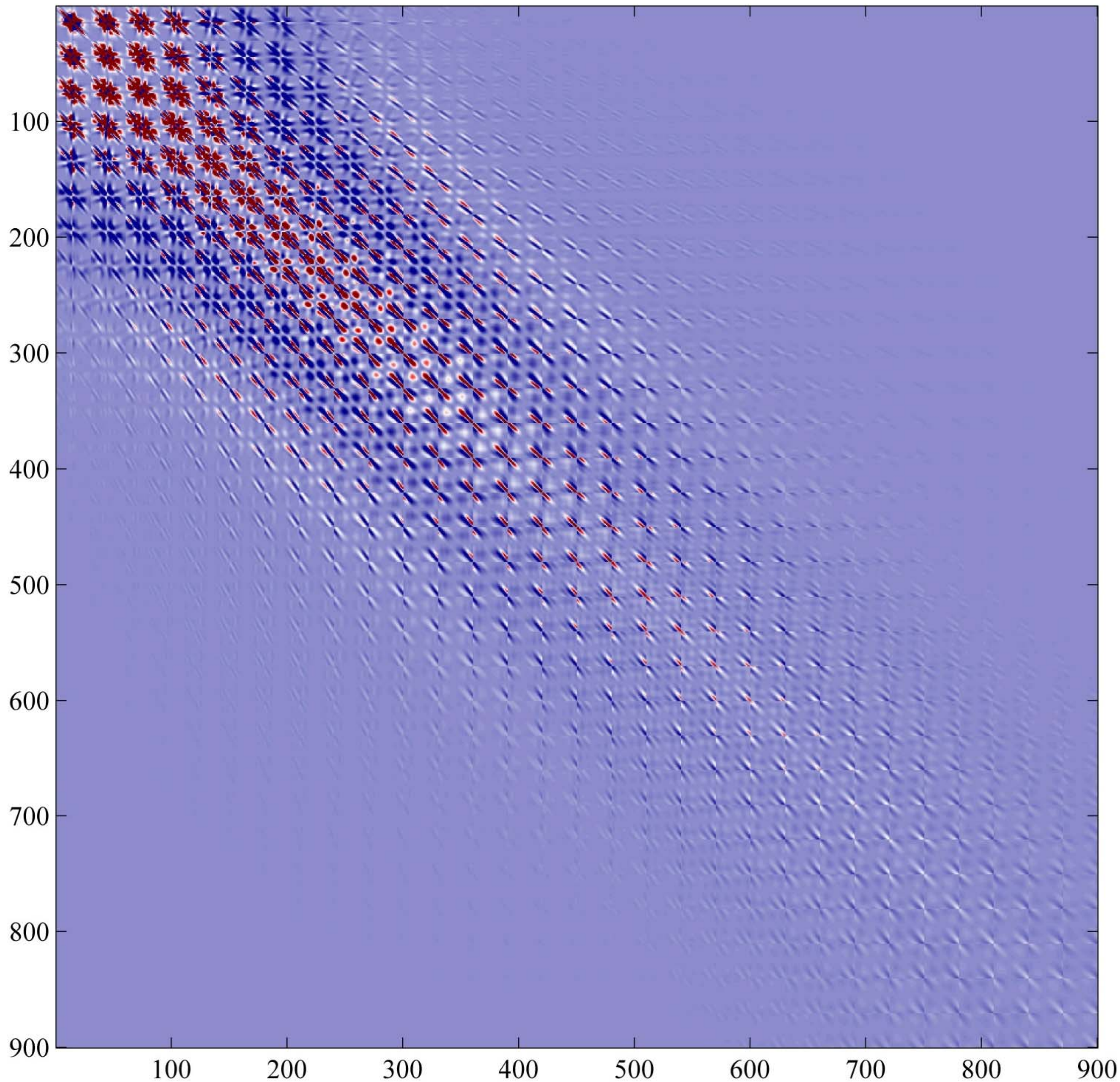

$$\frac{\partial^2 u}{\partial c_{11}^2}$$

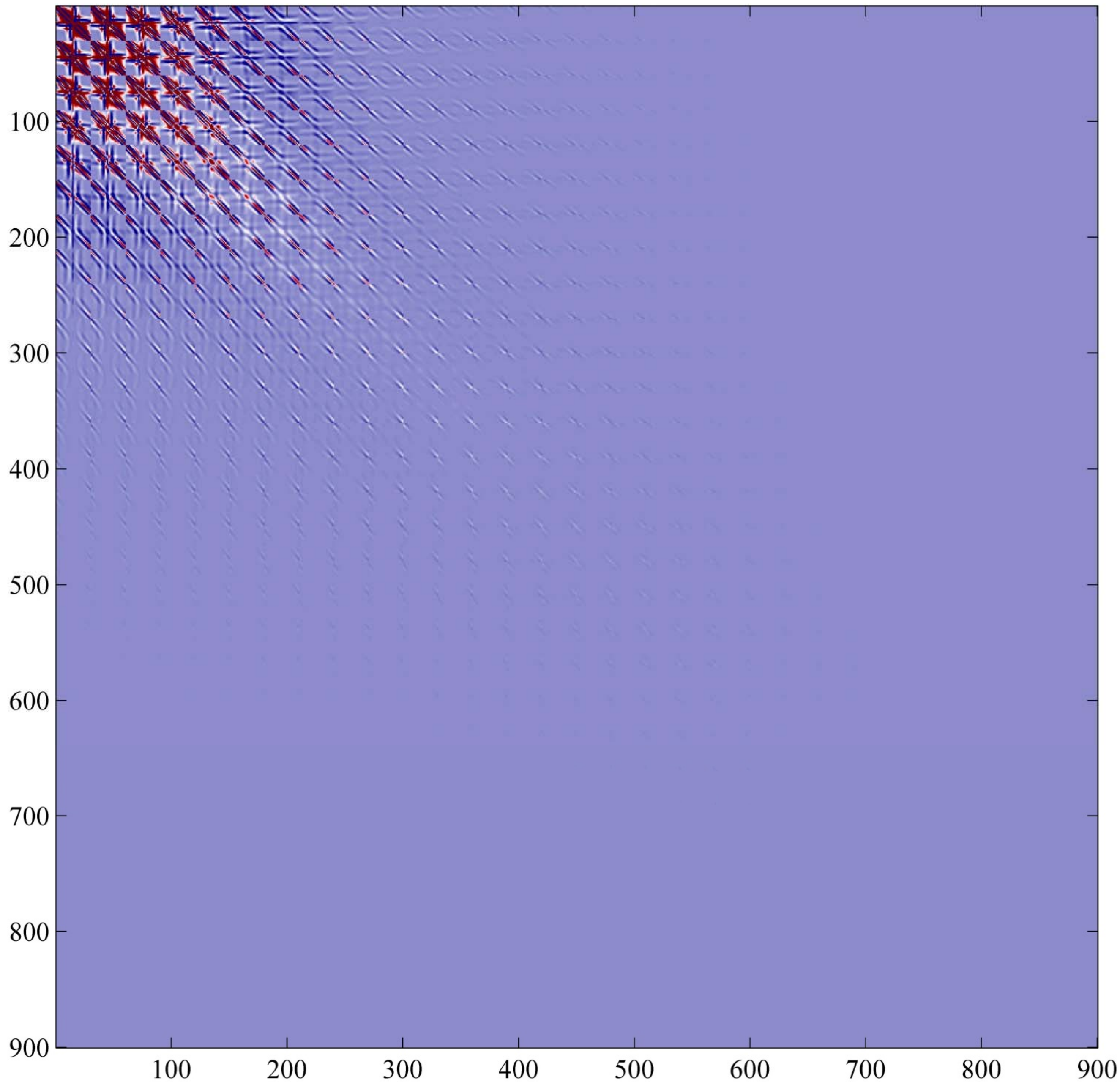

$$\frac{\partial^2 u}{\partial c_{13}^2}$$

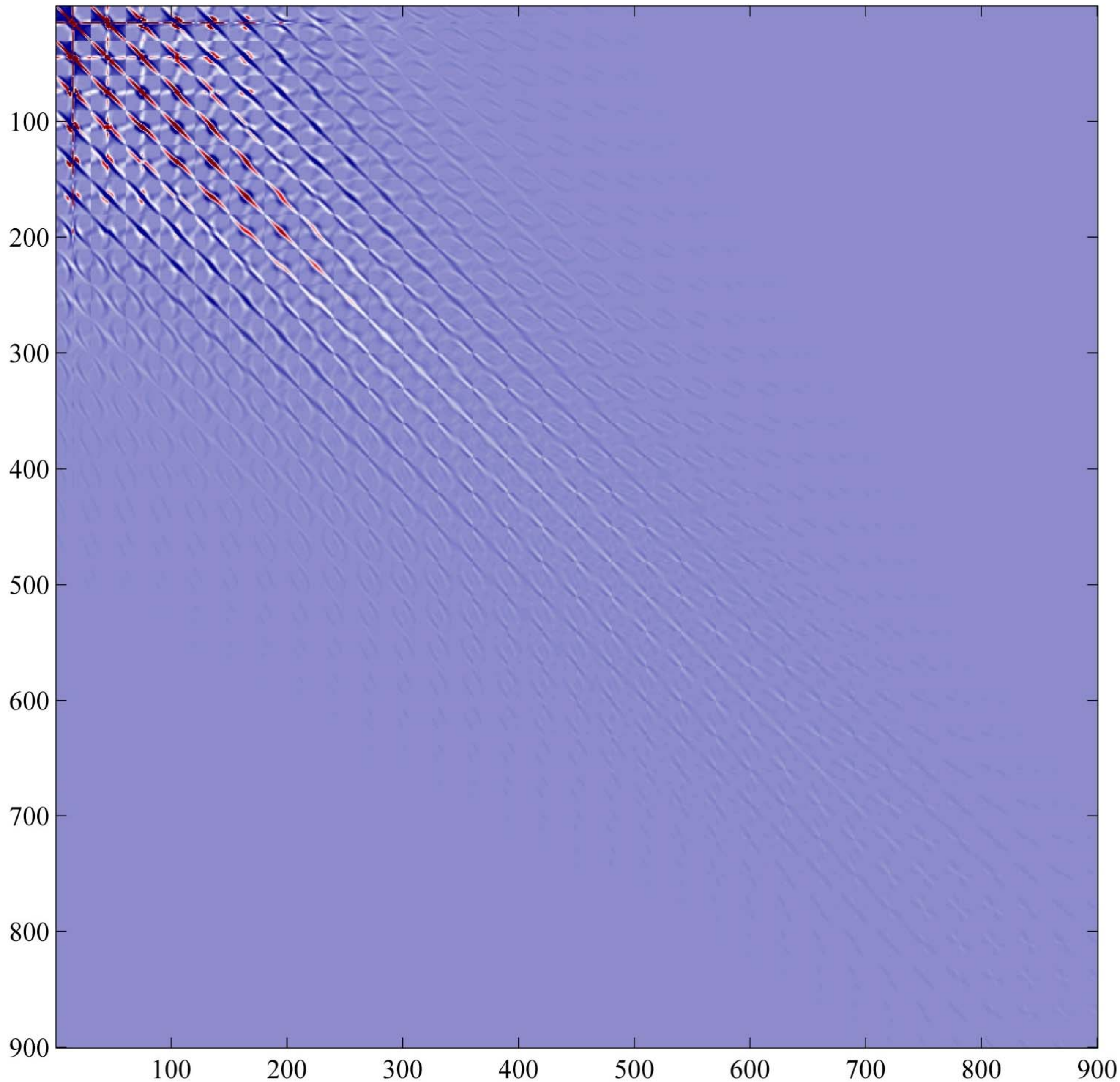

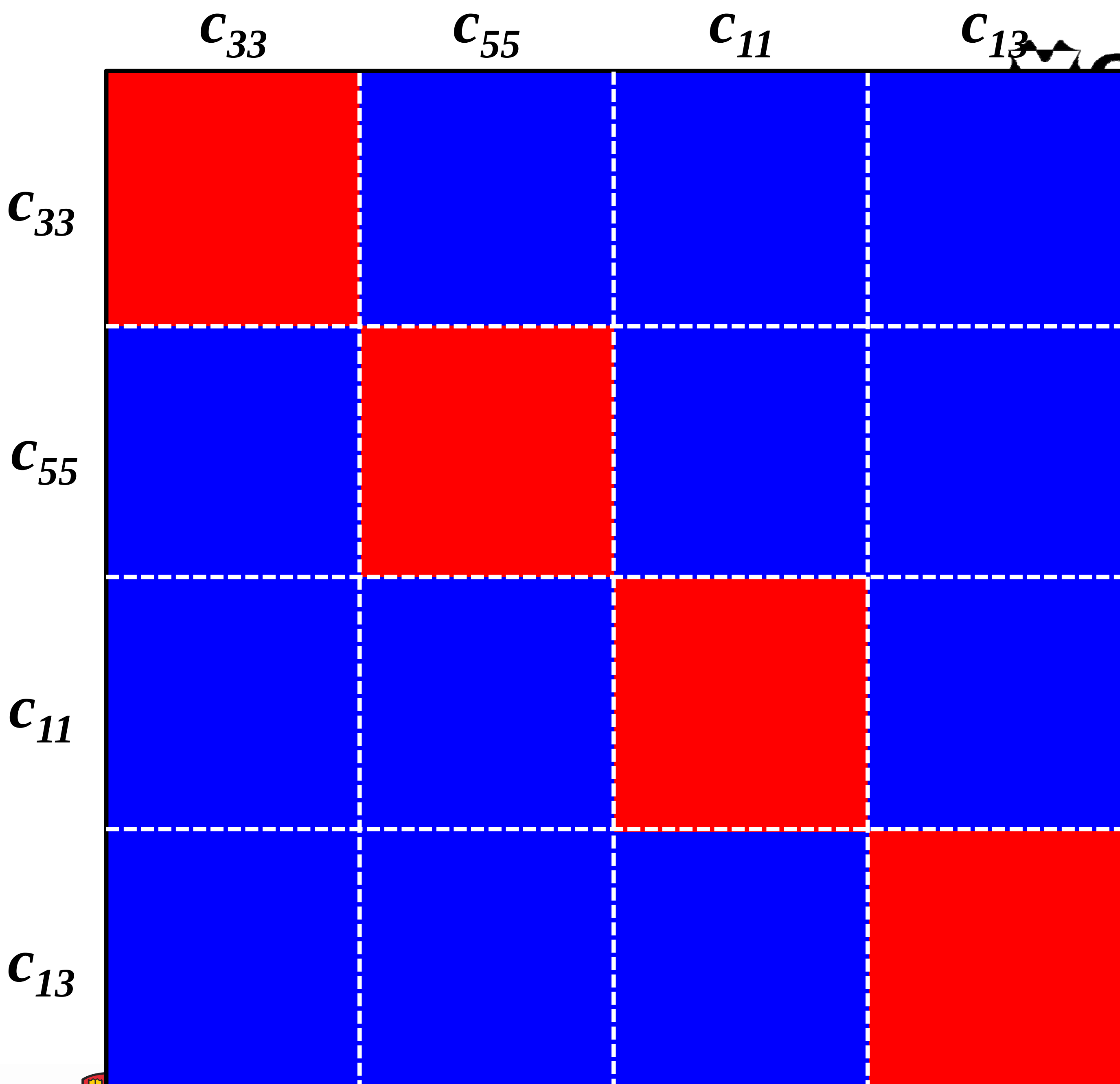

Crosstalk Block Matrices

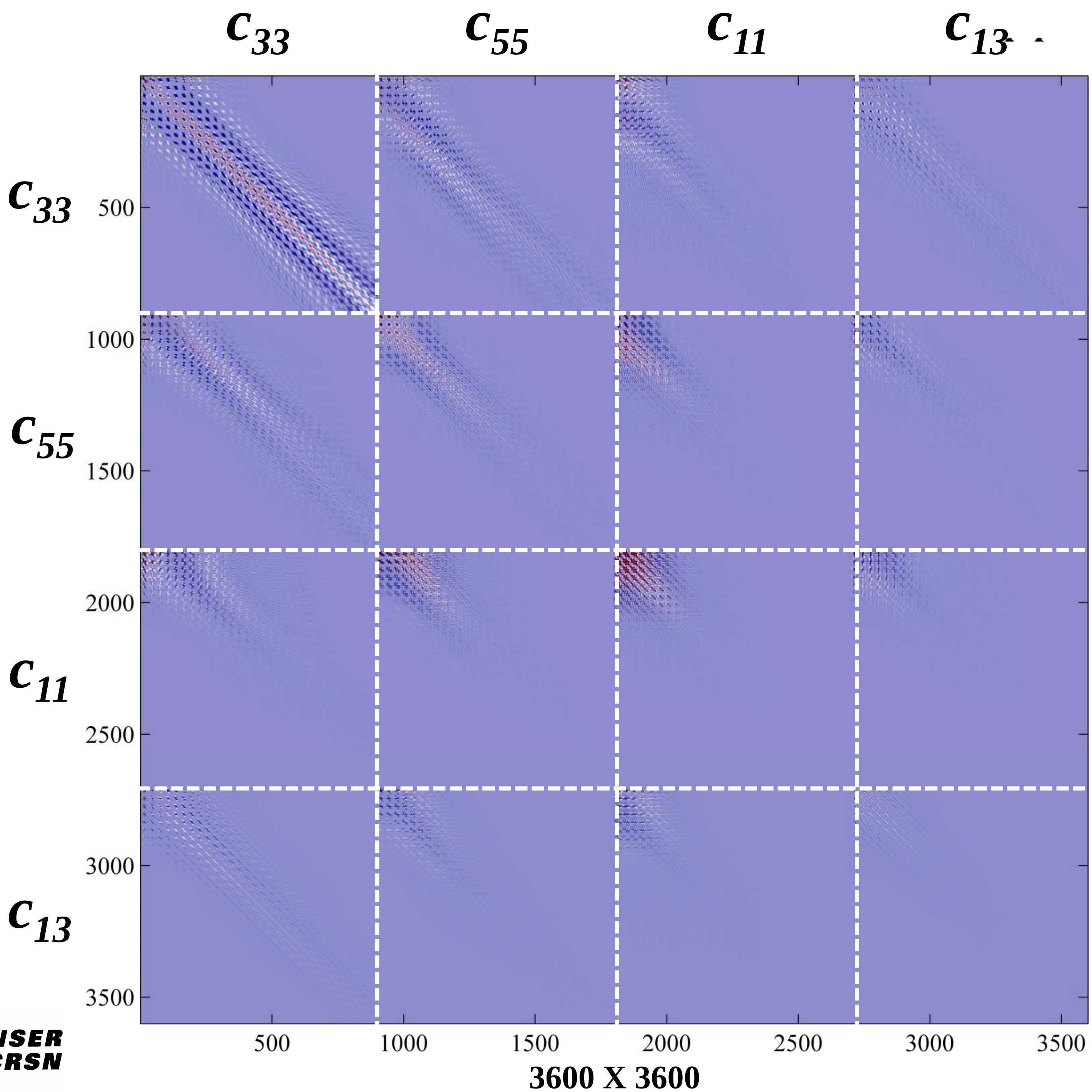

c_{33}
c_{55}
c_{11}
c_{13}
500
1000
1500
2000
2500
3000
3500
3600 X 3600

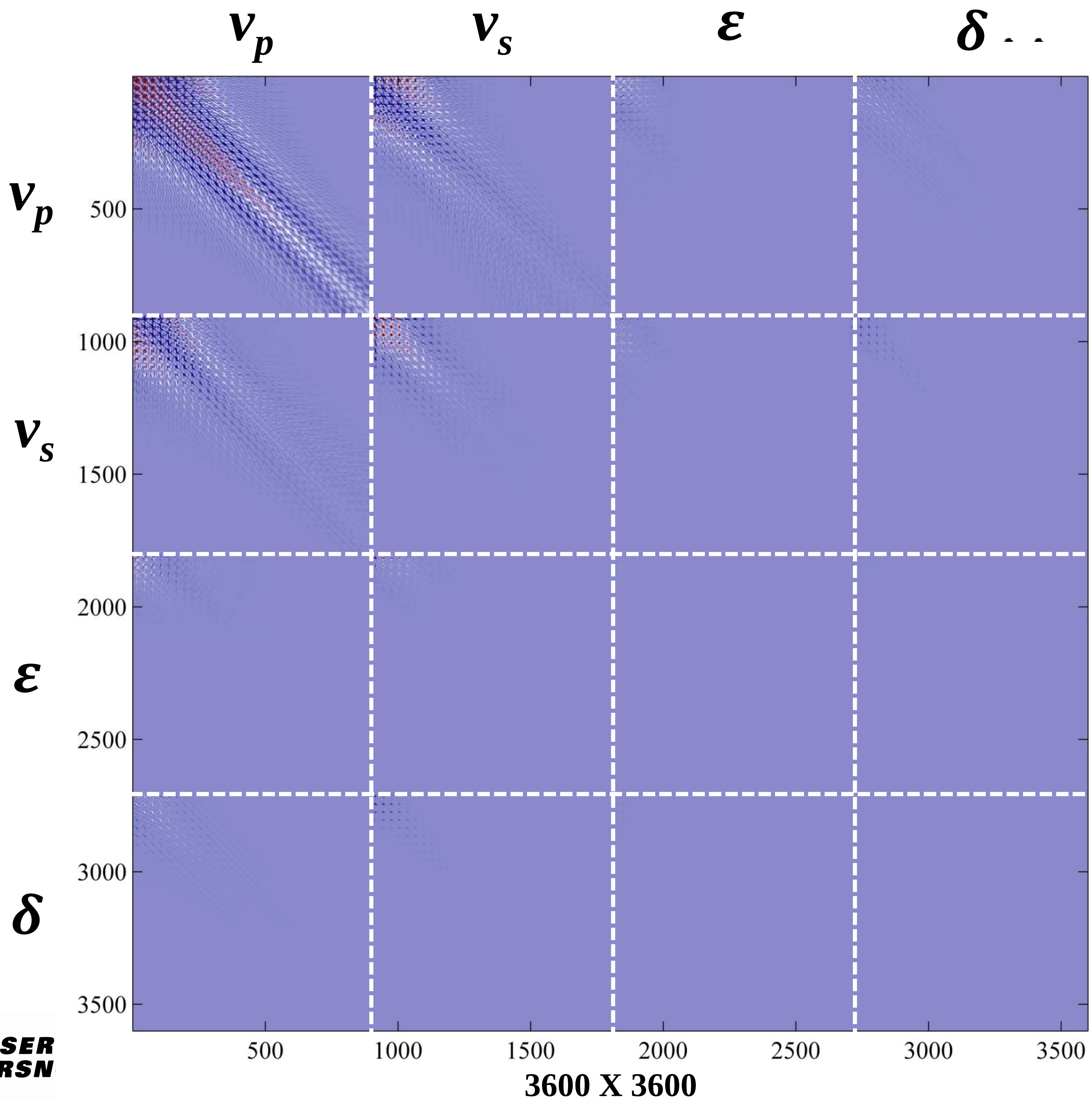
v_p
v_s
ε
δ
500
1000
1500
2000
2500
3000
3500
3600 X 3600

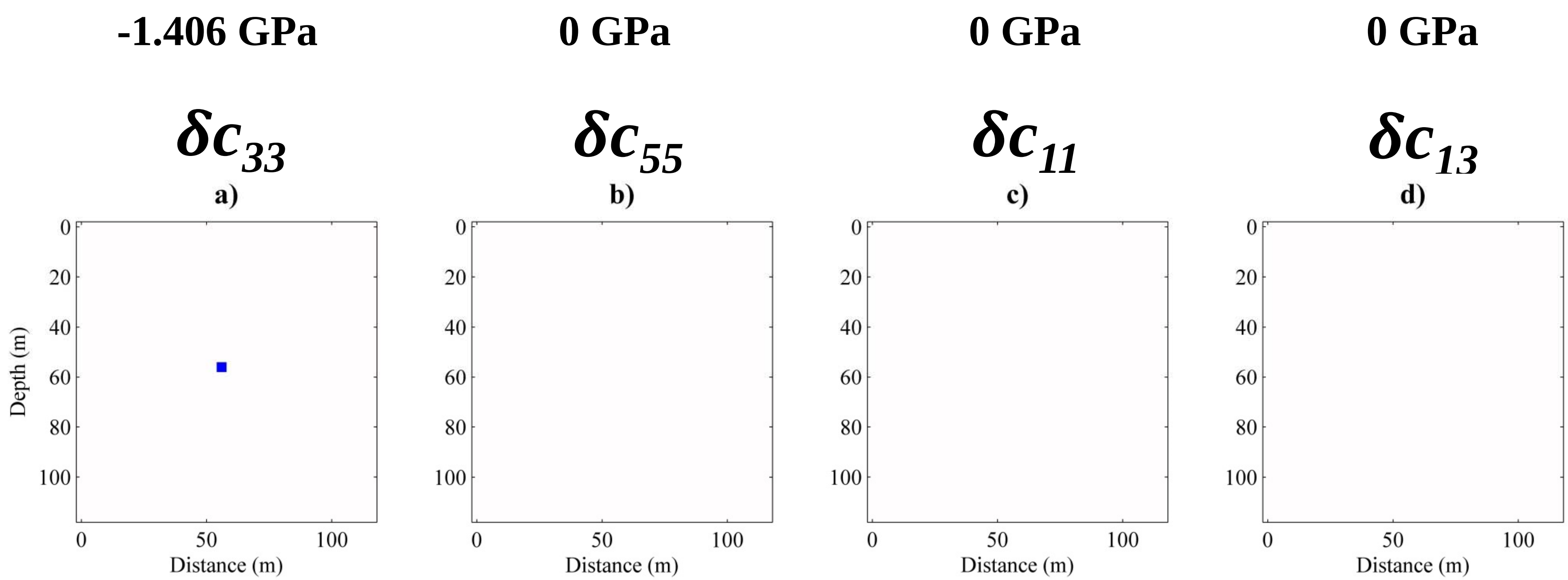

Mono Parameter True Model Perturbation

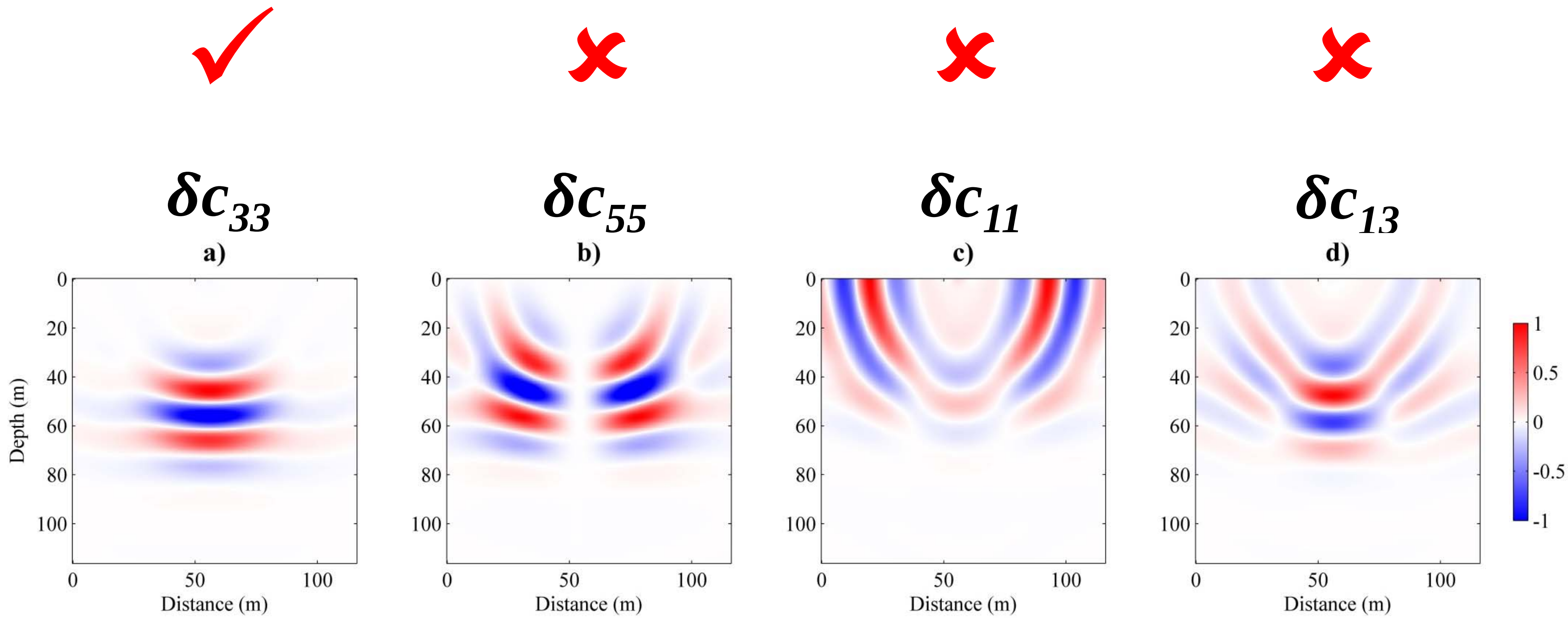

Gradient Suffered from Cross-talk

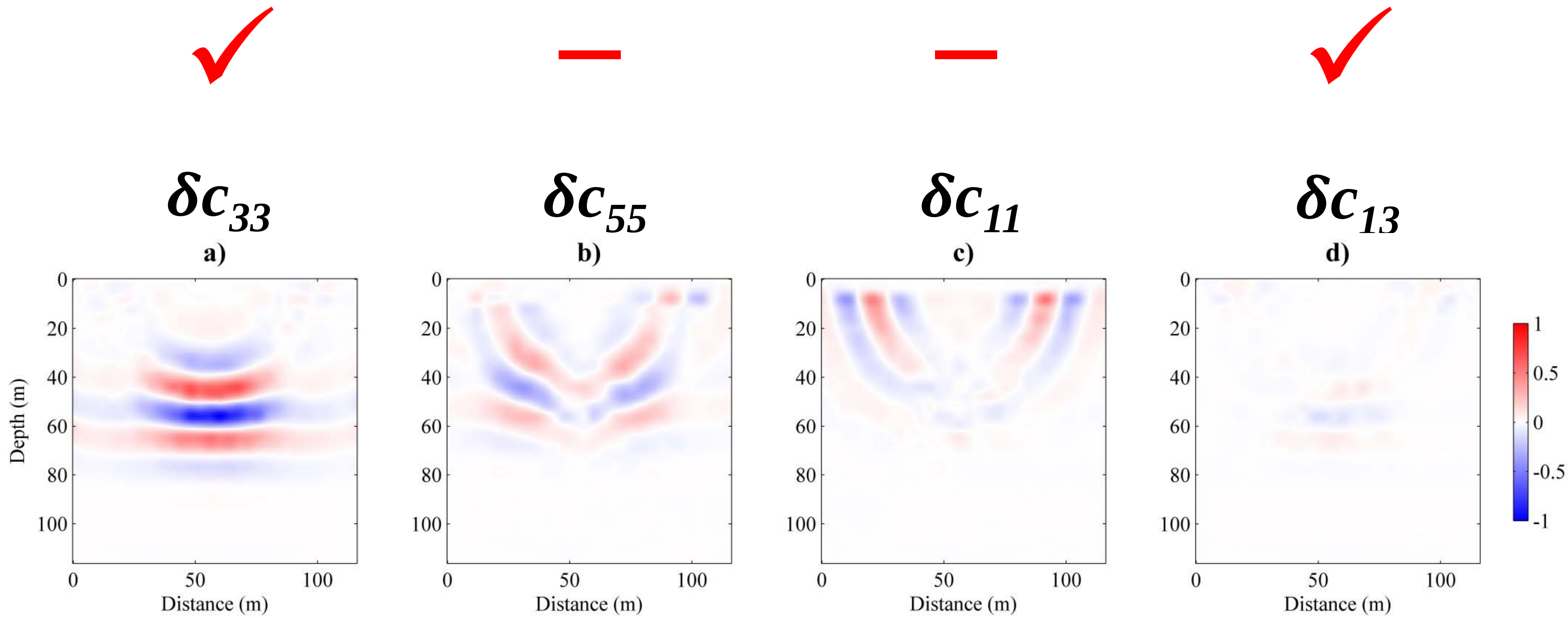

Gradient with Parameter-type Hessian Approximation Precondition

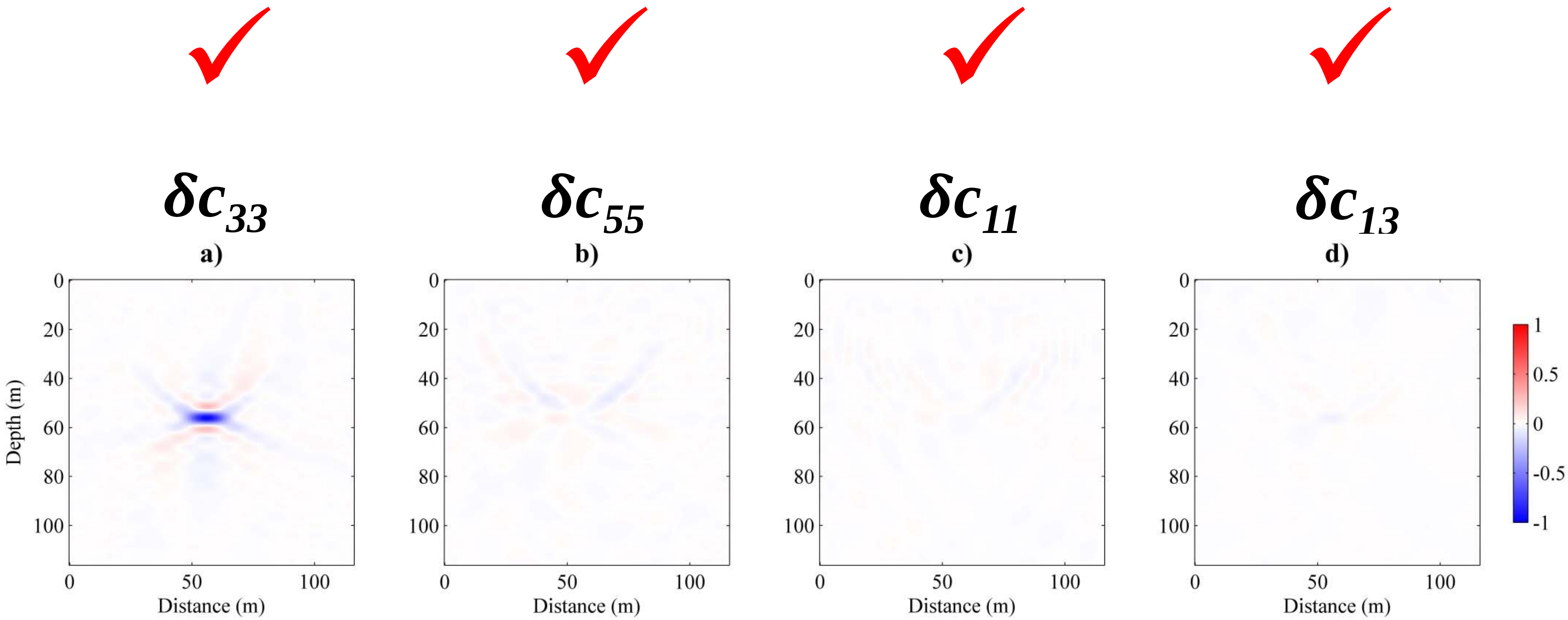

Gradient with Multi-parameter Hessian Precondition

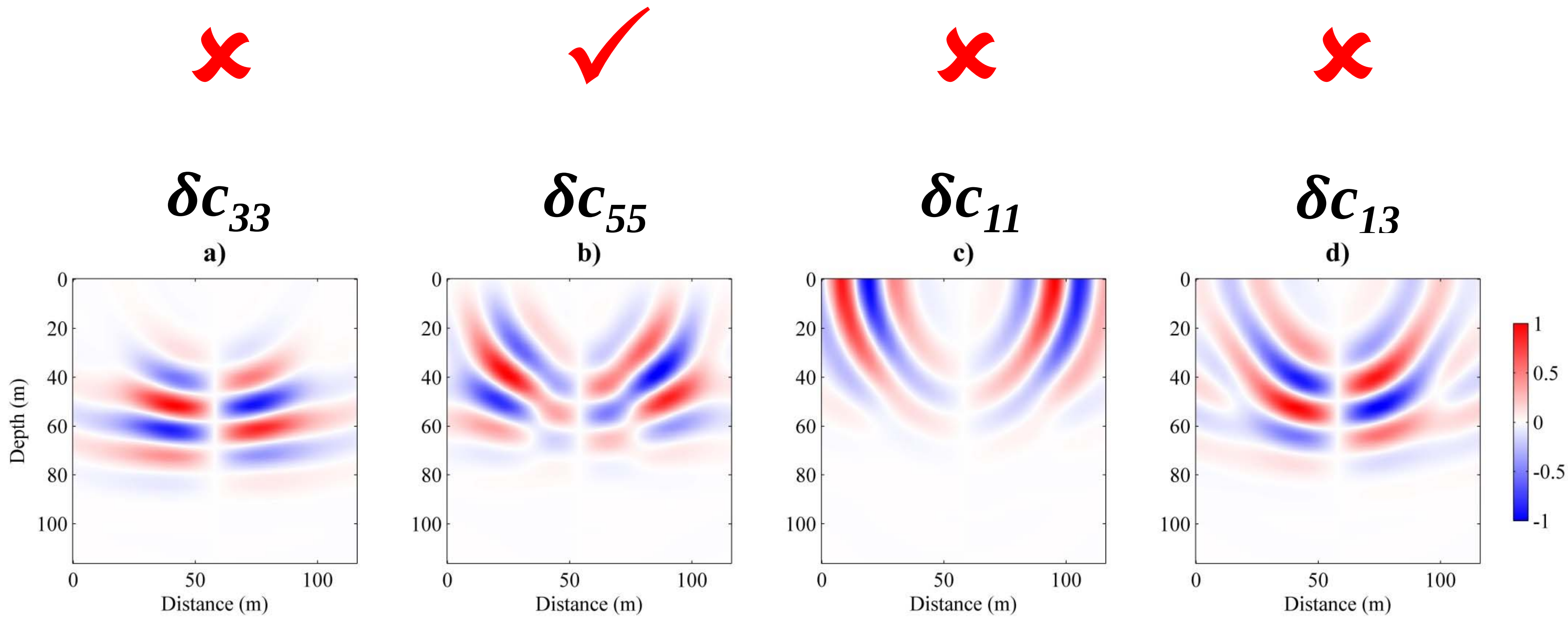

Gradient Suffered from Cross-talk

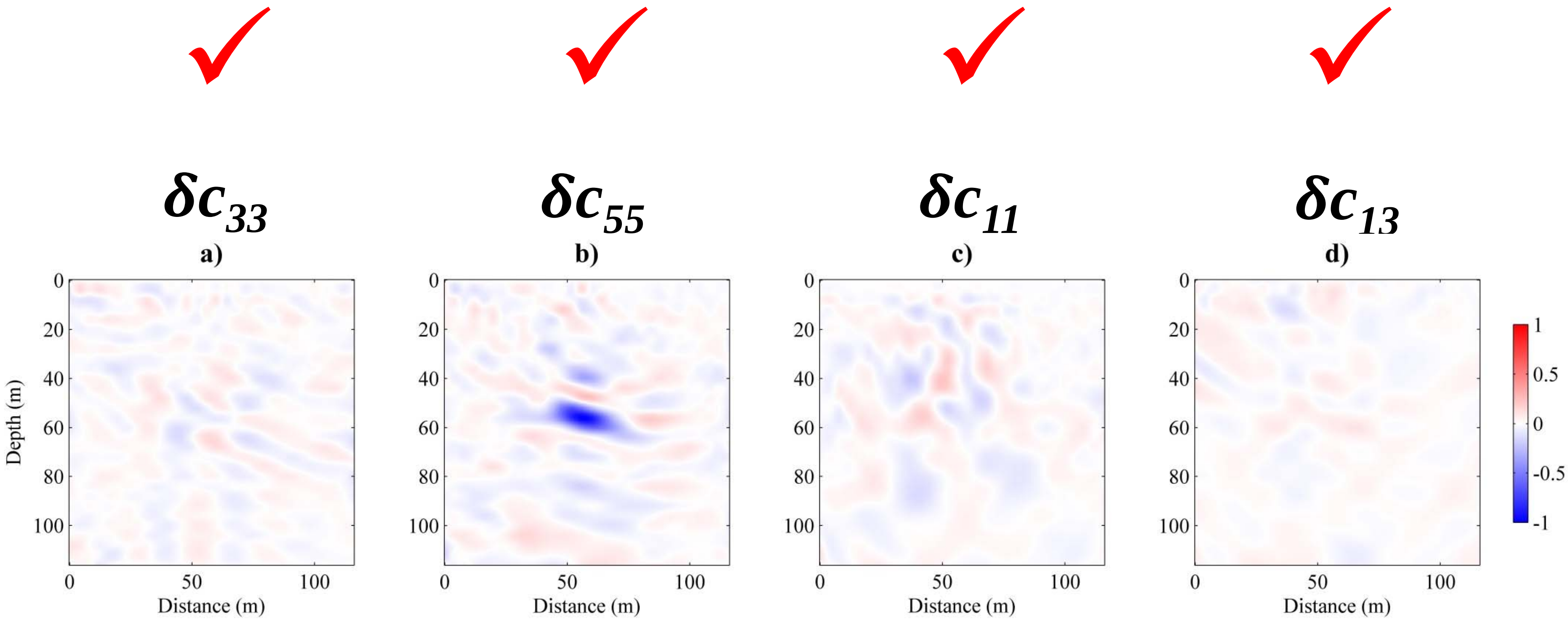

Gradient with Multi-parameter Hessian Precondition

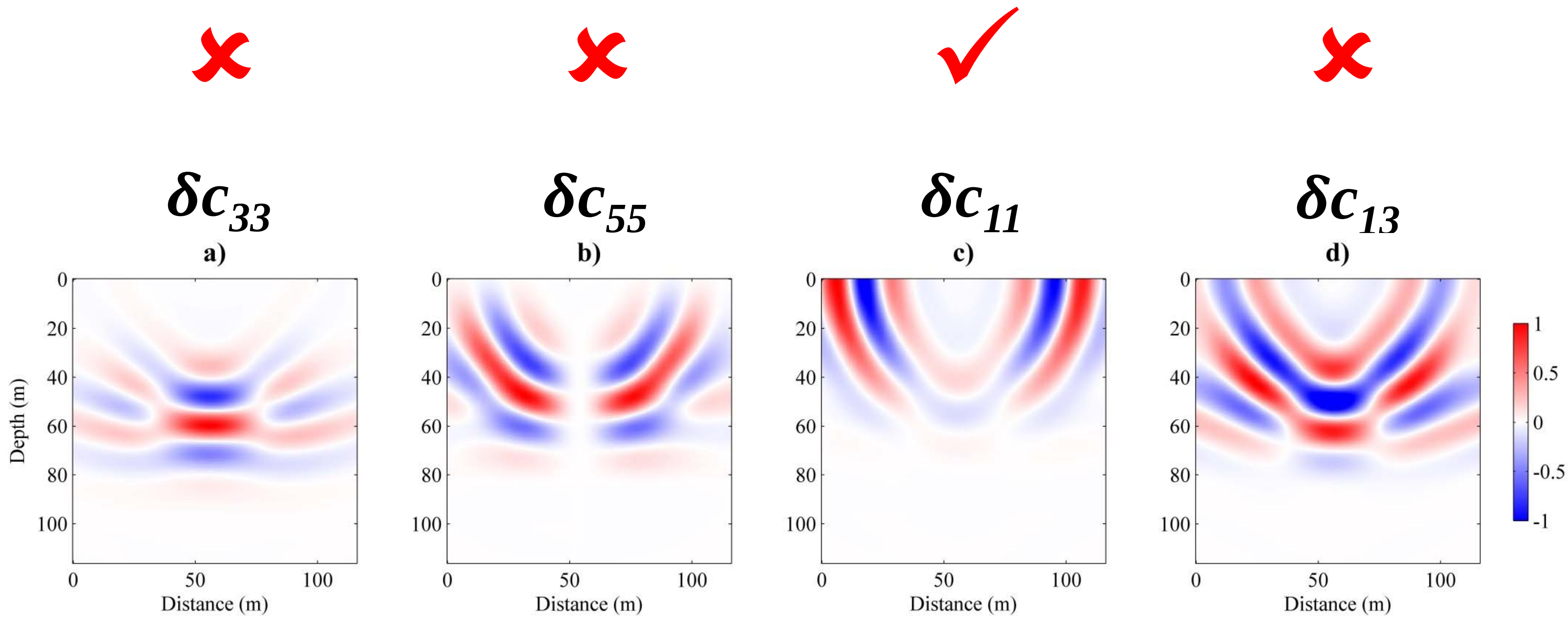

Gradient Suffered from Cross-talk

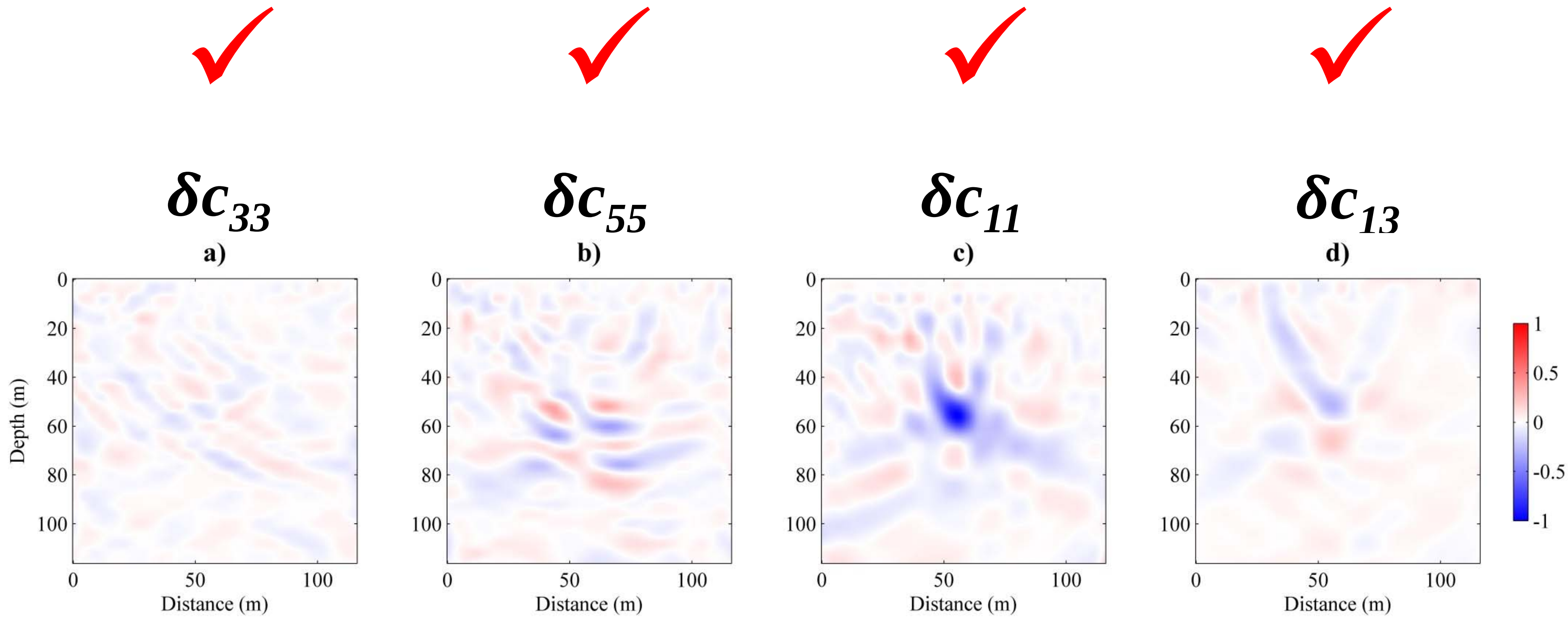

Gradient with Multi-parameter Hessian Precondition

-1.406 GPa | -0.632 GPa | -1.406 GPa | -0.142 GPa

δc_{33} | δc_{55} | δc_{11} | δc_{13}

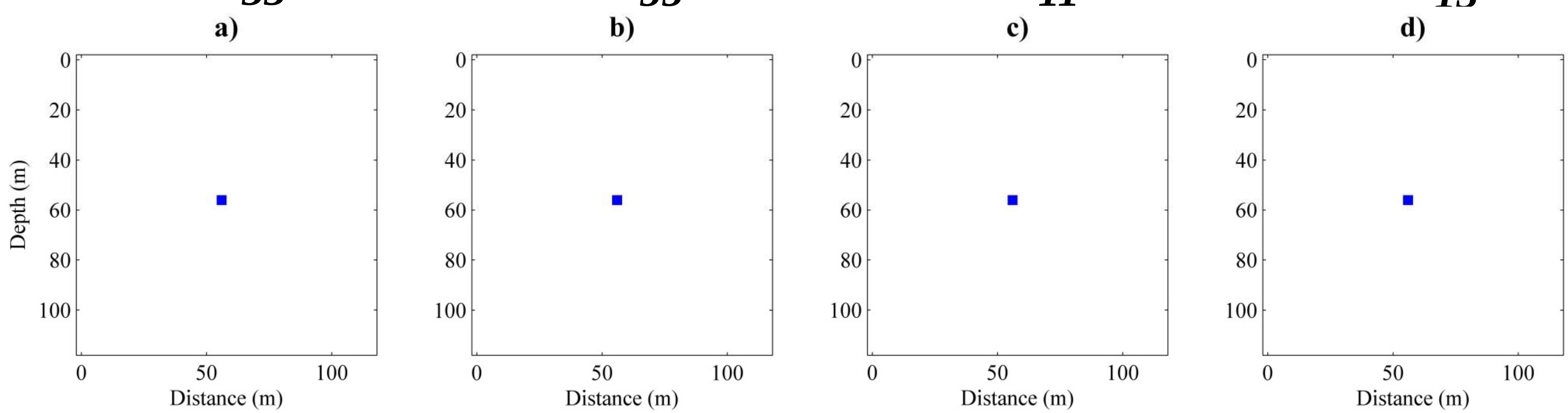

True Model Perturbation

δc_{33} δc_{55} δc_{11} δc_{13}

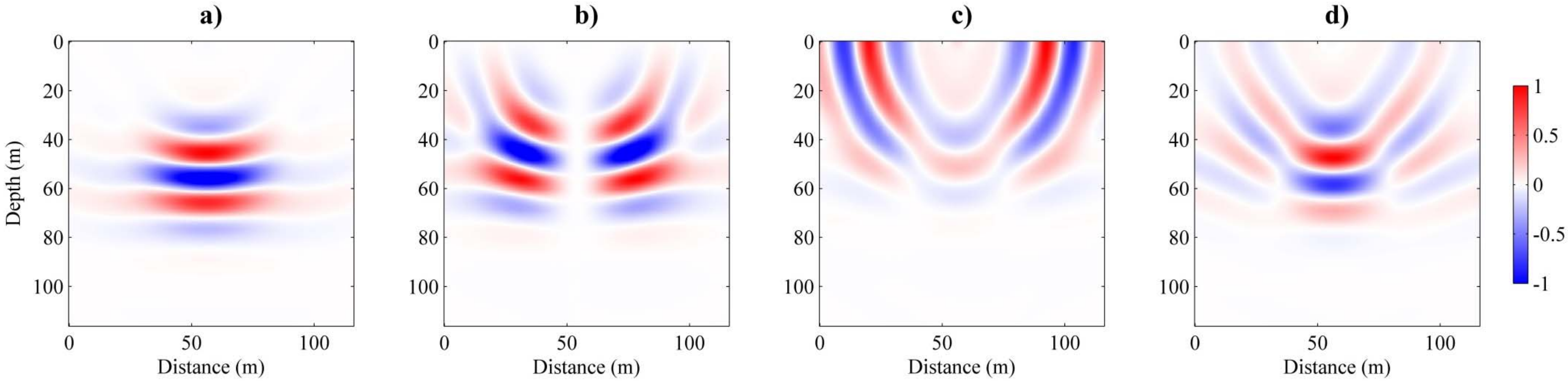

Gradient without Precondition

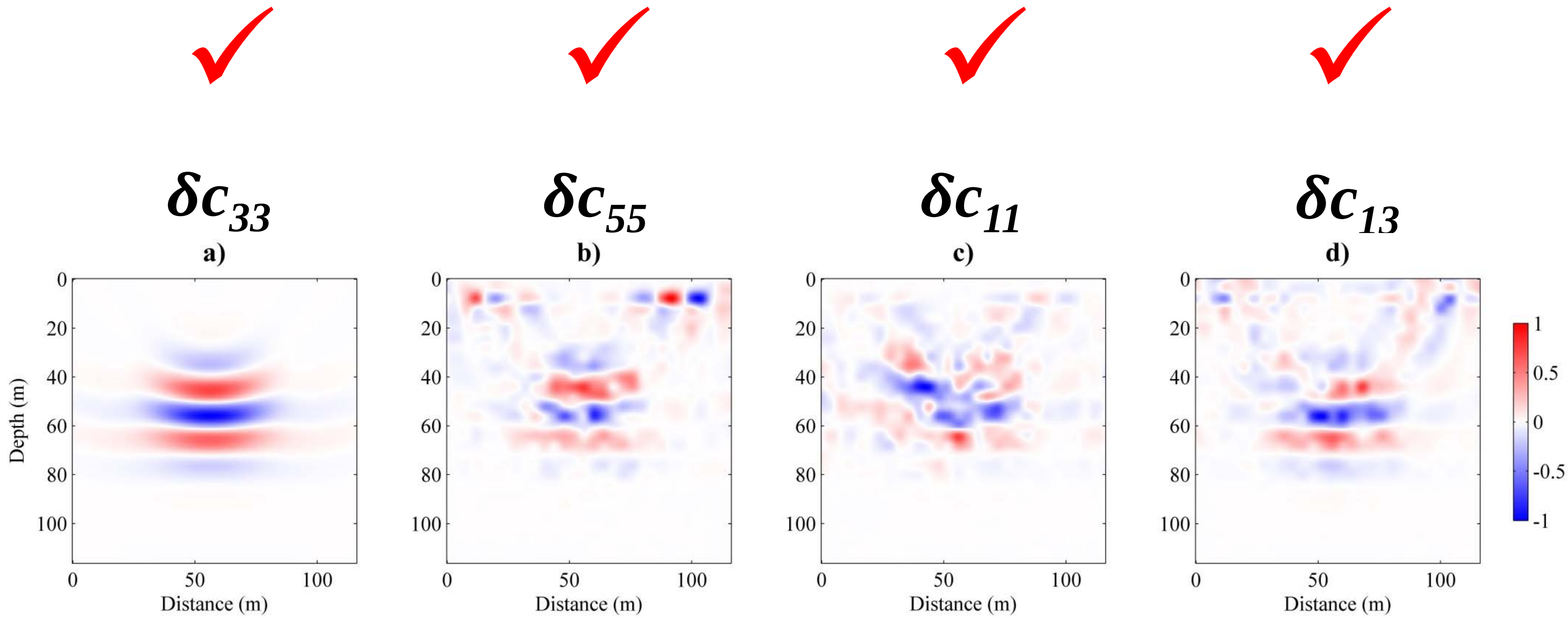

Gradient with Parameter-type Hessian Precondition with Cross-talk

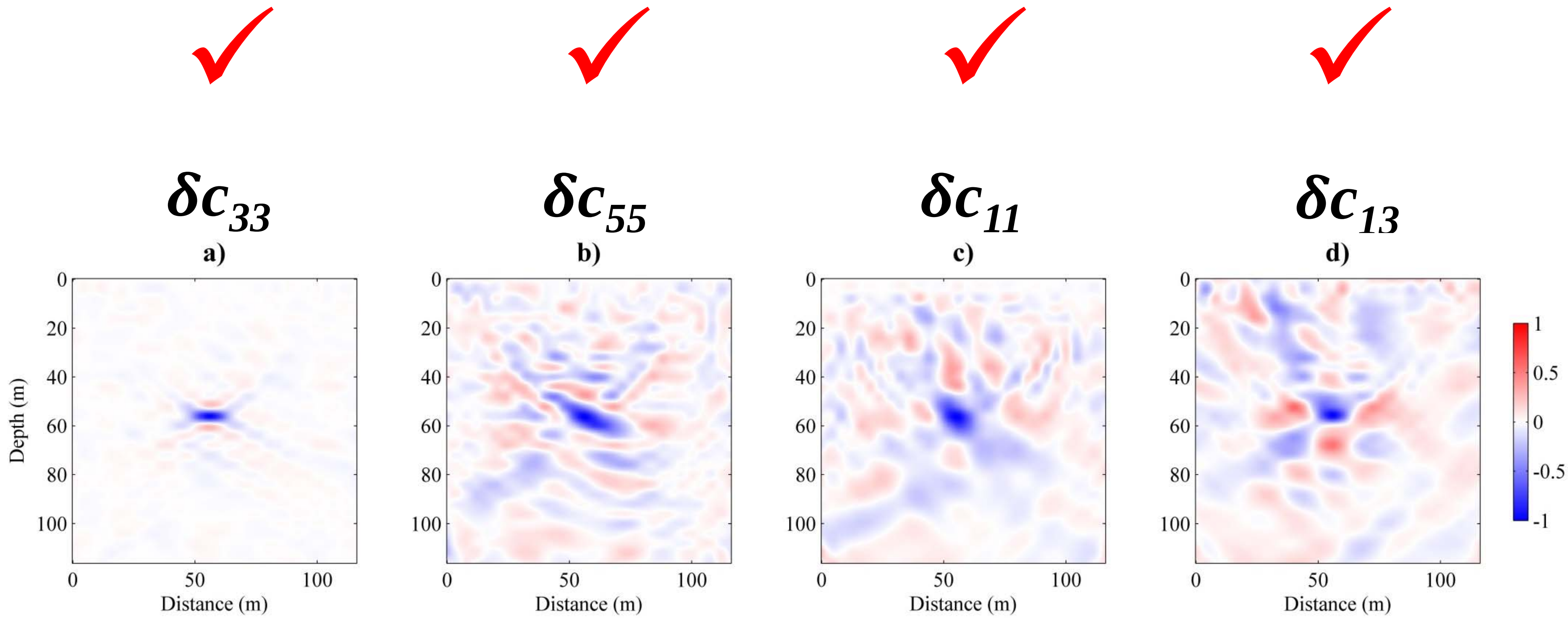

Gradient with Approximate Hessian Precondition with Cross-talk

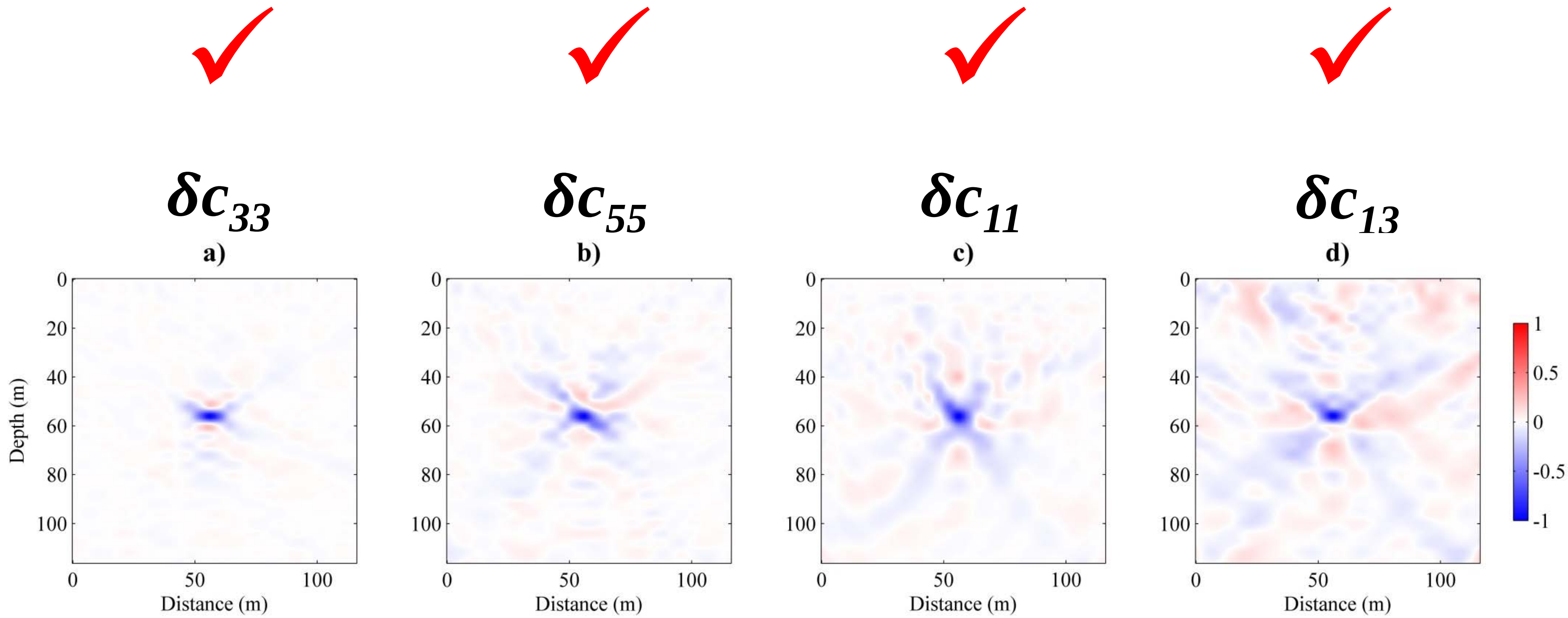

Gradient with Approximate Hessian Precondition with Cross-talk (3 Sources)

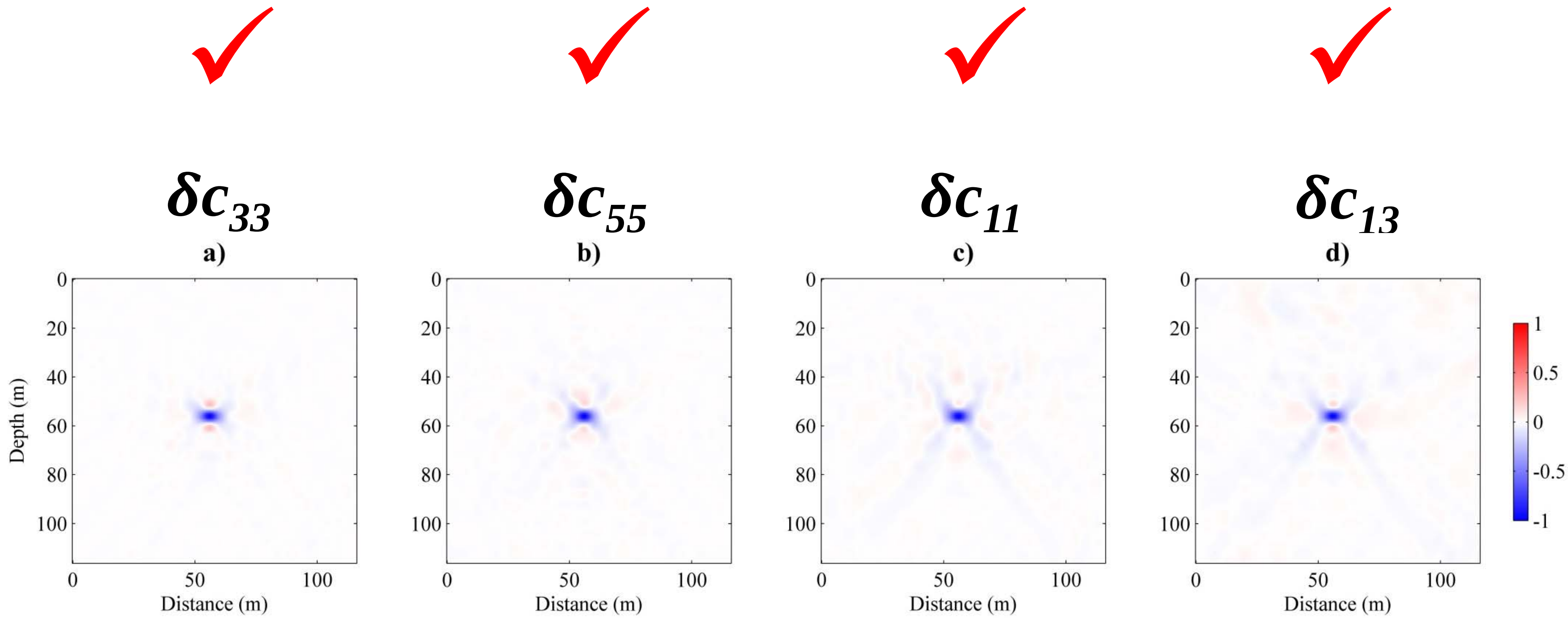

Estimated Model Perturbation with Approximate Hessian Precondition with Cross-talk (3 Sources and 3 Iterations)

Conclusions:

- ❖ Elastic constants in fractured media can be estimated directly using FWI.
- ❖ Multi-parameter FWI suffers from cross-talk.
- ❖ Inversion sensitivity analysis and scattering patterns control the cross-talk .
- ❖ Multi-parameter Hessian can suppress cross-talk.
- ❖ Target-oriented Gauss-Newton multi-parameter FWI is appropriate extension.
- ❖ Analysis for multi-component and multi-azimuth data (3D) is also needed.

Acknowledgements

- All CREWES Sponsors and Researchers
- Tiansheng Chen (SINOPEC)
- Di Yang (MIT & Exxon Mobil), Sam Ahmad Zamanian (MIT & Shell), Sudhish Bakku (MIT), Stephen Brown (MIT) and Xuan Feng (Jilin University)

Thank You !